09,04

Structural and spectral characteristics of $La_{0.99-x}Tb_xEu_{0.01}BO_3$ orthoborates and energy transfer from Tb^{3+} to Eu^{3+}

© S.Z. Shmurak, V.V. Kedrov, A.P. Kiselev, T.N. Fursova, I.I. Zver'kova

Osipyan Institute of Solid State Physics RAS,
Chernogolovka, Russia

E-mail: shmurak@issp.ac.ru

Received July 14, 2022
Revised August 7, 2022
Accepted August 8, 2022

The structure, infrared (IR) absorption spectra, luminescence spectra (SL), and luminescence excitation spectra (LES) of $La_{0.99-x}Tb_xEu_{0.01}BO_3$ orthoborates synthesized at 970°C at $0 \le x \le 0.99$ were studied. An increase in x leads to the successive emergence of three structural states of these compounds. At $0 \le x \le 0.2$, orthoborates have an aragonite structure; then, at $0.2 < x < 0.89$, they become two-phase and contain the aragonite and vaterite phases. At $0.89 \le x \le 0.99$, the compounds have a vaterite structure. A correspondence between the structure and spectral characteristics of these compounds was established. It is shown that in $La_{0.99-x}Tb_xEu_{0.01}BO_3$ orthoborates, as well as in $La_{0.99-x}Y_xEu_{0.01}BO_3$, the band with $\lambda_{ex} = 369$ nm ($^7F_0 \rightarrow {}^5D_2$) in the LES and the band in the wavelength range of 577−582 nm ($^5D_0 \rightarrow {}^7F_0$) in the SL of these compounds can serve as indicators of the structural state of the sample. In the SL of the samples containing the aragonite and vaterite phases, two bands corresponding to these structures were simultaneously observed for the first time. It was established that the luminescence of Eu^{3+} ions in $La_{0.99-x}Tb_xEu_{0.01}BO_3$ orthoborates, which occurs when the sample is excited by light in the absorption bands of Tb^{3+} ions, is due to the transfer of the electron excitation energy from Tb^{3+} ions to Eu^{3+} ions. The efficiency of this process in $La_{0.9}Tb_{0.09}Eu_{0.01}BO_3$ samples with an aragonite structure is 86%.

Keywords: rare earth orthoborates, crystal structure, X-ray diffraction analysis, IR spectroscopy, luminescence spectra, phosphors for LEDs.

DOI: 10.21883/PSS.2022.12.54393.438

1. Introduction

A number of fundamental characteristics of polymorphic compounds used as phosphors and materials for LEDs depend on their structural state. For example, the band gap (E_g) of $LuBO_3$ samples having the structure of vaterite and calcite is 7.0 and 6.4 eV, respectively [1,2]. The different spectral composition of photoluminescence of the vaterite and calcite modifications of $LuBO_3$(Eu) causes the red and orange luminescence characteristic of these structures, respectively [3–7]. Significant differences are also observed in the luminescence excitation spectra (LES) of various structural modifications of these compounds [4–7]. The LES of the most intense luminescence bands $LuBO_3$(Eu) contain a charge transfer band (CTB) with a maximum at ~ 238 nm for the vaterite structure and at ~ 250 nm — for calcite, as well as resonant bands of Eu^{3+} ions, the most intense of which is the band with $\lambda_{ex} \sim 394$ nm. The cardinal difference between the LES of the vaterite and calcite phases $LuBO_3$(Eu) lies in the ratio of the intensities of the CTB and the resonant bands. In the LES of the orthoborate $LuBO_3$(Eu), having a vaterite structure, the CTB amplitude ($\lambda_{ex} = 238$ nm) is $\sim 1.3-1.5$ times more intense than the band 394 nm, while in the LES calcite modification of these samples, the CTB exceeds the most intense resonant band $\lambda_{ex} = 394$ nm by more than 30 times. In orthoborates $InBO_3$(Eu) having a calcite structure, CTB is also more than 30 times more intense than the band 394 nm. The presence of a dominant charge transfer band in the LES is an important characteristic of the calcite modification of compounds $ReBO_3$, where Re = Lu, In [4–7].

In the luminescence spectrum of borates of rare earth ions doped with Tb^{3+} — $ReBO_3$(Tb), where Re — Lu, Eu, Gd, Y the narrow bands with $\lambda_{max} = 542.3$ nm have the greatest intensity for the vaterite modification and $\lambda_{max} = 541.8$ and 549.5 nm for the calcite modification, corresponding to the transition $^5D_4 \rightarrow {}^7F_5$ [4,8–10].

In the luminescence excitation spectrum of the calcite modification $LuBO_3$(Tb), four bands are observed in the short-wavelength area of the spectrum with $\lambda_{ex} = 235.7$, 260.2, 273.5 and 284.3 nm (transition $4f^8 \rightarrow 4f^75d^1$) and a narrow resonant band with $\lambda_{ex} = 378.5$ nm ($^7F_6 \rightarrow {}^5D_3$). The amplitude of the most intense shortwave band (235.7 nm) is about an order of magnitude higher than the amplitude of the band 378.5 nm. The luminescence excitation spectrum of the vaterite modification $LuBO_3$(Tb) differs significantly from the LES of the calcite structure. It consists of two wide shortwave bands with $\lambda_{ex} = 242$ and 285 nm ($4f^8 \rightarrow 4f^75d^1$) and a number of narrow bands in wavelength areas 300−375 nm, the most intense of which are at 304, 317, 354, 361, 363.5, 370.6, 374, 378.5, 382.8 nm and a separately located band 488.6 nm ($^7F_6 \rightarrow {}^5D_4$) [4,8–10].

In compounds containing several optically active rare earth ions, the process of electron excitation energy transfer from one center (donor — D) to another (acceptor — A) can be carried out. Electron excitation energy is transferred not by the process of photon emission (adsorption), but as a result of radiationless energy transfer due to Coulomb interaction between the donor and acceptor (Ferster mechanism of energy transfer). Two conditions must be met for fulfilling the energy transfer process: 1) donor emission spectrum (D) must be in the spectral range of acceptor absorption (A); 2) distance between the donor and acceptor must be not more than the („threshold") distance R. It should be noted that energy transfer in various compounds takes place when distances between the donor and acceptor are in the range of $5-50$ Å [3,11–16]. The result of the energy transfer process from the donor to the acceptor is the appearance of the acceptor glow when the sample is excited in the absorption band of the donor. As a result of this process, the intensity of the luminescence of the acceptor A can significantly increase in comparison with the intensity of the luminescence of A during its resonant excitation [3.11]. Electron excitation energy transfer was studied for a whole range of compounds doped with different rare-earth ions.

In the studies [17–20] it is shown that the luminescence intensity of ions Tb^{3+} (I_{Tb}) in compounds $ReBO_3(Ce, Tb)$, where $Re = Lu$, Y, Gd, when excited by light corresponding to the maximum excitation of the luminescence of Ce^{3+} ions ($\lambda_{ex} \sim 340$ and ~ 370 nm for calcite and vaterite modifications, respectively), more than ~ 40 times exceeds I_{Tb} with resonant excitation of ions Tb^{3+} ($\lambda_{ex} = 378.5$ nm). Such a significant increase in the intensity of the luminescence of terbium ions is due to the high efficiency of the transfer of the energy of electronic excitation from the ions Ce^{3+} to Tb^{3+} ($\eta \sim 80\%$) in these compounds [17–19]. It should be noted that the efficiency of energy transfer from the ions Ce^{3+} to Tb^{3+} in the compound $Ba_3Gd(PO_4)_3(Ce, Tb)$ $\eta \sim 79\%$ [21] is close to the values of η for cerium and terbium-doped lutetium, yttrium and gadolinium borates. The maximum („threshold") distance (R), at which excitation can be transferred from cerium to terbium, for borates $YBO_3(Ce, Tb)$ and $LuBO_3(Ce, Tb)$ is equal to ~ 16 and ~ 18 Å respectively [17–20]. It should be noted that the value of R for the compound $Ba_3Gd(PO_4)_3(Ce, Tb)$ is ~ 16 Å [21]. Close values of „threshold" distances at which energy is transferred from Ce^{3+} to Tb^{3+}, as well as values for efficiency of energy transfer from Ce^{3+} to Tb^{3+}, for various compounds means that the energy transfer from Ce^{3+} to Tb^{3+} is virtually independent from the matrix where cerium and terbium ions are located.

At the same time, these compounds have a strong dependence of glow intensity of ions Tb^{3+} (I_{Tb}) on their concentration: I_{Tb} decreases $\sim$ in 2 times in relation to the maximum value upon an increase in Tb^{3+} concentration to ~ 20 at.% [19,20].

The transfer of electron excitation energy from ions Tb^{3+} to Eu^{3+} was observed in a number of compounds: in molybdates [22] and tungstates [23] of rare earth elements, in $Tb(OH)_3(Eu)$ samples, $SrTiO_3(Tb, Eu)$ [24,25], orthoborates $YBO_3(Tb + Eu)$ [26] and $MeBO_3(Tb, Eu)$, where $Me = La$, Gd, In [27]. The highest efficiency of energy transfer (η) from Tb^{3+} to Eu^{3+} was observed in the samples of $Tb(OH)_3 : Eu^{3+}$. When the concentration of ions Eu^{3+} increased from 0.03 to 3 mol.%, the value of η increases in these samples from 67 to 99% [24].

In the study [27], luminescence spectra and luminescence excitation spectra of $La_{1-x-y}Tb_xEu_yBO_3$ compounds were studied. The concentration of one of the activator ions (x, y) was maintained in the range from 1 to 4 mol.%, and the other was adjusted so that the total doping level ($x + y$) was 5 mol.%. It is shown that in compounds doped with europium and terbium, intense luminescence of Eu^{3+} ions is observed, while the luminescence intensity of Tb^{3+} ions is extremely low. This is due, as the authors of [6] believe, to the transfer of energy from Tb^{3+} ions to Eu^{3+}.

The energy transfer from Ce^{3+} ions to Yb^{3+} in $LaBO_3(Ce, Yb)$ samples was investigated in [28]. It is shown that the efficiency of electron excitation energy transfer from Ce^{3+} ions to Yb^{3+} (η) in compounds $La_{0.92-y}Ce_{0.08}Yb_yBO_3$ increases with increasing concentration of Yb^{3+} and at $y \sim 0.02$ approaches saturation. At $y = 0.02$ and 0.035, the values of $\eta \sim 60$ and 70%, respectively, which indicates a sufficiently high efficiency of energy transfer from ions Ce^{3+} to Yb^{3+} in $LaBO_3(Ce, Yb)$ orthoborates.

Lutetium borate ($LuBO_3$) has two stable structural modifications: vaterite, which is formed during the synthesis of $LuBO_3$ at $T = 750-850°C$, and calcite, which is formed at $T = 970-1100°C$ [29–31]. At the same time, orthoborates $ReBO_3$ (where Re — Tb, Eu, Gd, Y) have only one structural modification — vaterite [29,30,32]. Orthoborate $LaBO_3$ has two phase states: the low-temperature orthorhombic phase aragonite (SG $Pnam$) and the high-temperature monoclinic phase (SG $P2_1/m$), in which $LaBO_3$ passes at a temperature of 1488°C [31–35]. Lutetium ion in the structures of calcite, vaterite and aragonite surrounded by six, eight and nine oxygen atoms, respectively. Boron ions in calcite and aragonite structures have trigonal oxygen coordination — $(BO_3)^{3-}$ [36]. At the same time, three boron atoms with a tetrahedral environment by oxygen in the vaterite structure make up a $(B_3O_9)^{9-}$ group in the form of a three-dimensional ring [37].

Solid solution investigation $La_{0.98-x}Lu_xEu_{0.02}BO_3$ synthesized at $T = 970°C$ (the temperature of existence of the aragonite structure $LaBO_3$ and phases of calcite $LuBO_3$), showed that with an increase in the concentration of lutetium, there is a sequential change of three types of crystalline phases: aragonite, vaterite and calcite. Schematically, the process of alternating structural states in compounds $La_{0.98-x}Lu_xEu_{0.02}BO_3$ with increasing concentration Lu^{3+}

can be represented as follows:

aragonite (at $0 \le x < 0.15$) →
aragonite + vaterite ($0.15 \le x \le 0.8$) →
vaterite ($0.8 < x < 0.88$) →
vaterite + calcite ($0.88 \le x < 0.93$) →
calcite ($0.93 \le x \le 0.98$) [38].

The same sequence of changes in structural states is observed in orthoborates $Pr_{0.99-x}Lu_xEu_{0.01}BO_3$ [39] synthesized at $T = 970°C$ (the temperature of the existence of the aragonite structure $PrBO_3$ [40–42]). The only difference is that in orthoborates $Pr_{0.99-x}Lu_xEu_{0.01}BO_3$, single-phase vaterite is formed in a wider range of Lu^{3+} concentrations ($0.6 < x \le 0.8$) than in $La_{0.98-x}Lu_xEu_{0.02}BO_3$ ($0.8 < x < 0.88$). Thus, despite the fact that at $T = 970°C$ $ReBO_3$ (Re = La, Pr) has the structure of aragonite, and $LuBO_3$ — calcite, the structure transformation of orthoborates $Re_{0.99-x}Lu_xEu_{0.01}BO_3$ (Re = La, Pr) from aragonite to calcite is carried out through the formation of the vaterite phase. In connection with this circumstance, in the work [43], a study of a compound consisting of orthoborates having structures of aragonite ($LaBO_3$) and vaterite (YBO_3). It is shown that with an increase in the concentration of ions Y^{3+} in orthoborates $La_{0.99-x}Y_xEu_{0.01}BO_3$, the expected change of structural states occurs. At $0 \le x \le 0.1$ the compounds are single-phase and have the structure of aragonite (SG $Pnam$). At $0.1 < x \le 0.8$ samples are two-phase, they contain phases of aragonite and vaterite. At $0.8 < x \le 0.99$, orthoborates are single-phase with a vaterite structure (SG $P6_3/m$). An unambiguous correspondence has been established between the structure and spectral characteristics of the orthoborates $La_{0.99-x}Y_xEu_{0.01}BO_3$. It is shown for the first time that the band with $\lambda_{ex} = 369$ nm ($^7F_0 \to {}^5D_2$) in the luminescence excitation spectrum (LES) and the band in the wavelength range 577–582 nm ($^5D_0 \to {}^7F_0$) in the luminescence spectrum (LS) of $La_{0.99-x}Y_xEu_{0.01}BO_3$ compounds can serve as indicators of the structural state of the sample. The band with $\lambda_{ex} = 369$ nm is observed in the LES samples having a vaterite structure, while it is absent in samples with an aragonite structure. If the maximum of the band corresponding to the transition is in the LS $^5D_0 \to {}^7F_0$, is at wavelengths less than 580 nm, then the sample has an aragonite structure if λ is greater than 580 nm, then the sample has a vaterite structure.

It seems appropriate to establish how general the patterns obtained in the work [43] are. As noted, Tb, Eu, Gd orthoborates, as well as YBO_3, have only one structural modification — vaterite [29,30,32]. In this paper, studies of changes in the structure, IR spectra, luminescence spectra and luminescence excitation spectra of orthoborates $La_{0.99-x}Tb_xEu_{0.01}BO_3$ at $0 \le x \le 0.99$. Electron excitation energy transfer from ions Tb^{3+} to ions Eu^{3+} in these compounds has been studied. The correspondence between structure and spectral characteristics of these compounds was established. The ions Eu^{3+}, like in our previous research, were used as optically active and structure-sensitive labels in amounts not affecting the structural transformations of orthoborates.

2. Experimental procedures

2.1. Sample synthesis

Samples of polycrystalline powders of orthoborates of the compositions $La_{0.99-x}Tb_xEu_{0.01}BO_3$ were obtained by interaction of oxides of rare earth elements with a melt of potassium tetraborate by reaction:

$$(0.99 - x)La_2O_3 + xTb_2O_3 + 0.01Eu_2O_3 + K_2B_4O_7 = 2La_{0.99-x}Tb_xEu_{0.01}BO_3 + K_2B_2O_4.$$

The amount of potassium tetraborate taken into the reaction provided an excess of the boron-containing reagent relative to the stoichiometric amount by 10–20%. The initial compounds for orthoborate synthesis were potassium tetraborate tetrahydrate $K_2B_4O_7 \cdot 4H_2O$ and calibrated aqueous solutions of nitrates of rare earth elements. All the chemicals used corresponded to the qualification „AR grade".

Microcrystalline orthoborate powders were synthesized as follows. A weighed amount of potassium tetraborate tetrahydrate was placed in a ceramic round-bottomed cup, stoichiometric amounts of aqueous solutions of rare earth nitrates, taken in the required ratio, were added and thoroughly mixed. The resulting aqueous suspension was heated on a tile and water was distilled at low boiling. The resulting solid product was annealed at a temperature of 550°C for 20 min to remove water and nitrate decomposition products, after which it was thoroughly ground in an agate mortar. The resulting powder was transferred to a ceramic crucible and subjected to high-temperature annealing at $T = 970°C$ for 2 h. The annealing product was treated with aqueous solution of hydrochloric acid with the concentration of 5 wt.% for 0.2 h while constantly mixing on a magnetic mixer. Orthoborate polycrystals were isolated by filtering the obtained aqueous suspension, followed by washing with water, alcohol, and product drying on a filter. The obtained powders of polycrystals of orthoborates were finally dried in air at $T = 200°C$ for 0.5 h.

2.2. Research methods

X-ray diffraction studies were performed using a Rigaku SmartLab SE diffractometer with CuK_α radiation, $\lambda = 1.54178$ Å, 40 kV, 35 mA. Angular interval was $2\theta = 10–140°$. Phase analysis of the samples and calculation of lattice parameters were performed using the Match and PowderCell 2.4 programs.

Samples' IR spectra of absorption were measured using a Fourier-spectrometer VERTEX 80v in the spectral range of $400-5000\,cm^{-1}$, resolution being $2\,cm^{-1}$. For measurements, the polycrystal powders were ground in an agate mortar, and then were applied in a thin layer onto a crystalline polished substrate of KBr.

The sample morphology was studied using a Supra 50VP X-ray microanalyzer with an add-on for EDS INCA (Oxford).

Photoluminescence spectra and luminescence excitation spectra were studied on a unit that consisted of a light source — DKSSh-150 lamp, two MDR-4 and MDR-6 monochromators (spectral range is 200−1000 nm, dispersion is 1.3 nm/mm). The luminescence was recorded by means of FEU-106 photomultiplier (spectral sensitivity range is 200−800 nm) and an amplification system. The MDR-4 monochromator was used to study the samples luminescence excitation spectra, the MDR-6 monochromator was used to study luminescence spectra.

The spectral and structural characteristics, as well as the morphology of the samples, were studied at room temperature.

3. X-ray diffraction studies

Diffractograms of powder samples of the studied compounds $La_{0.99-x}Tb_xEu_{0.01}BO_3$ and their phase composition at $0 \le x \le 0.99$ are shown in Fig. 1, 2 and in Table 1. At $0 \le x < 0.2$ the samples are single-phase and have aragonite structure, SG $Pnam$ N 62 (PDF 12-0762), $Z = 4$.

In the range $0.2 < x < 0.89$, the samples are two-phase — along with the structure of aragonite, a phase of vaterite is observed. At $0.89 \le x \le 0.99$, the samples are single-phase with a vaterite structure, SG $P6_3/m$ N 176, $Z = 2$ (PDF 01-080-3937).

In the range of concentrations of ions Tb^{3+} $0 \le x \le 0.2$ in single-phase samples with an aragonite structure, a monotonous decrease in the volume of the unit cell occurs with an increase of x (Fig. 3). This indicates the substitution of ions La^{3+}, having an ionic radius of 1.1148 Å, with ions Tb^{3+}, which have a smaller ionic radius (0.9565 Å) [44]. The maximum possible dissolution of ions Tb^{3+} in the aragonite phase $La_{0.99}Eu_{0.01}BO_3$ is ~ 27 at.% (Fig. 2). The composition of the resulting solid solution is $\sim La_{0.72}Tb_{0.27}Eu_{0.01}BO_3$. With further doping, additional terbium is not included in the structure of aragonite, but is consumed to increase the amount of phase vaterite.

In the two-phase area (aragonite + vaterite), the volume of the unit cell of each of these phases does not change, only a quantitative change in the ratio of aragonite and vaterite occurs (Fig. 3).

When doping $Tb_{0.99}Eu_{0.01}BO_3$ with lanthanum, which has a larger ionic radius compared to Tb^{3+}, an increase in the volume of the vaterite unit cell in single-phase samples is observed with an increase in the concentration of La^{3+}, which indicates the dissolution of lanthanum in the vaterite structure (Fig. 3). The maximum possible dissolution of ions La^{3+} in the vaterite phase is ~ 14 at.% (Fig. 2). The composition of the farming solid solution is $\sim La_{0.14}Tb_{0.85}Eu_{0.01}BO_3$.

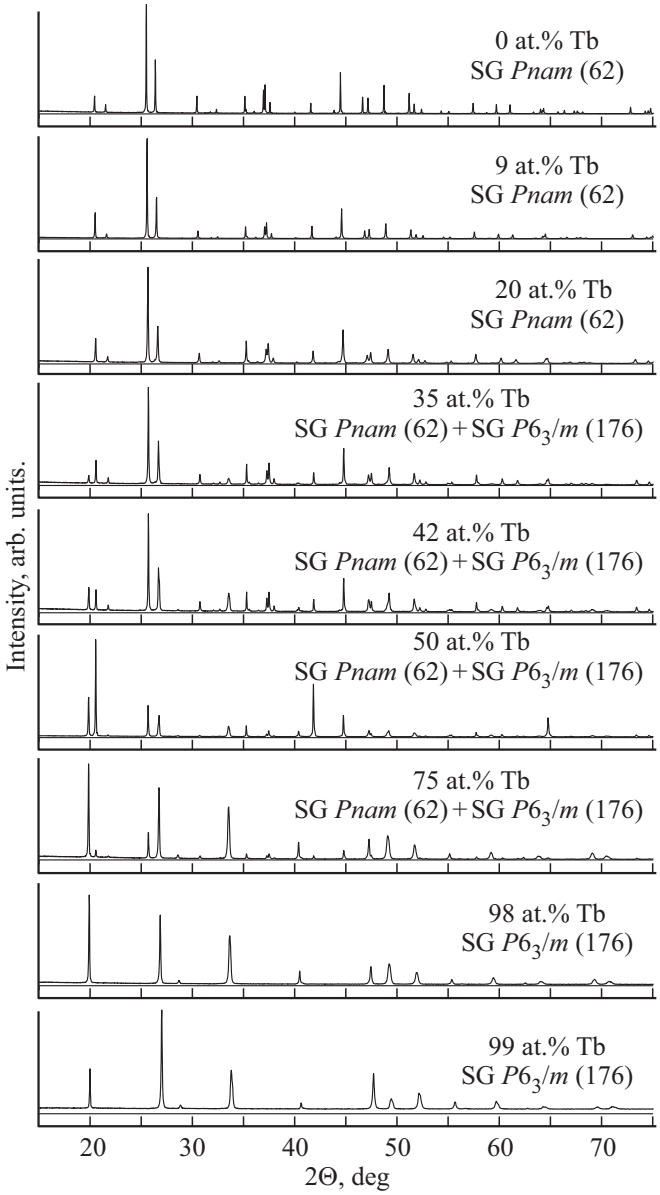

Figure 1. Diffractograms of samples $La_{0.99-x}Tb_xEu_{0.01}BO_3$.

Thus, in orthoborates $La_{0.99-x}Tb_xEu_{0.01}BO_3$, as well as in compounds $La_{0.99-x}Y_xEu_{0.01}BO_3$ [43], we can distinguish three areas in which there are certain structural states: at $0 \le x \le 0.2$ the solid solution $La_{0.99-x}Tb_xEu_{0.01}BO_3$ has the structure of aragonite, then in the range $0.2 < x < 0.89$ the samples are two-phase — along with the structure of aragonite phase of vaterite is observed, and at $0.89 \le x \le 0.99$ the samples are single-phase with a vaterite structure.

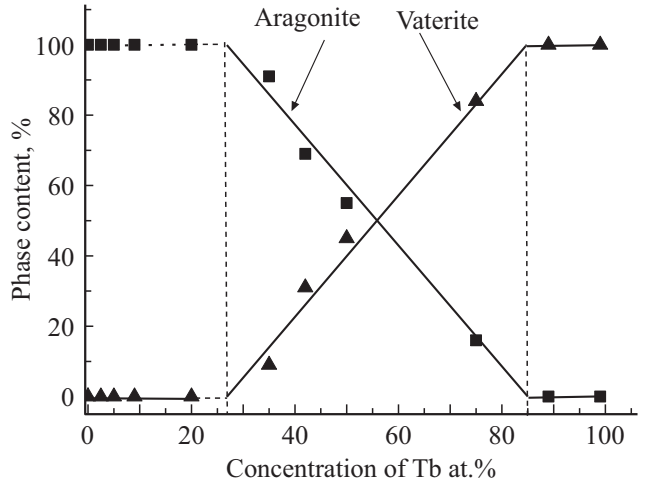

Figure 2. Phase composition of orthoborates $La_{0.99-x}Tb_xEu_{0.01}BO_3$ depending on the ratio of rare earths in the charge at $0 \le x \le 0.99$: square — aragonite, triangle — vaterite.

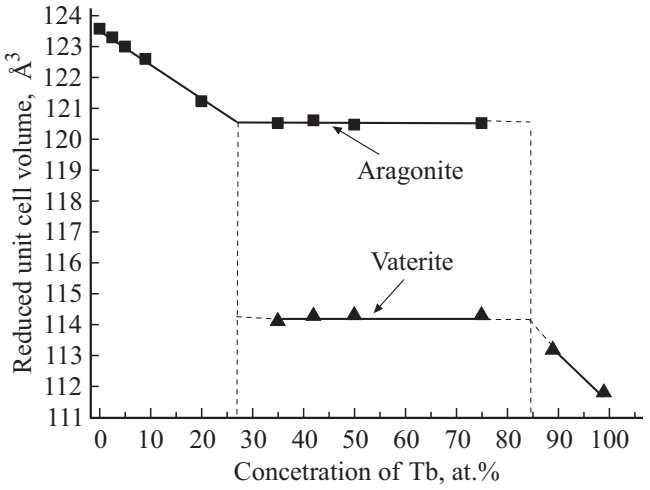

Figure 3. Volumes of elementary cells of aragonite and vaterite in the orthoborate $La_{0.99-x}Tb_xEu_{0.01}BO_3$ at $0 \le x \le 0.99$, reduced to $Z = 2$: square — aragonite, triangle — vaterite.

4. Morphology of samples

Samples $La_{0.99-x}Tb_xEu_{0.01}BO_3$ having at $0 \le x \le 0.2$ the structure of aragonite (Table 1), contain mainly microcrystals of size $\sim 0.5-3\,\mu$m. These samples also contain a small number of microcrystals of large sizes $\sim 10\,\mu$m (Fig. 4, *a*). In samples $La_{0.64}Tb_{0.35}Eu_{0.01}BO_3$, which contain 91% aragonite (A) and 9% vaterite (V) and $La_{0.49}Tb_{0.5}Eu_{0.01}BO_3$ (55% A and 45% V) both flat and volumetric microcrystals with a size of $2-10\,\mu$m, that do not have a certain cut are observed which have numerous continuity violations (Fig 4, *b, c*). The same uncut microcrystals with a large number of defects and cracks of size $2-10\,\mu$m are observed in samples $La_{0.24}Tb_{0.75}Eu_{0.01}BO_3$ (15% A, 85% V) and $La_{0.1}Tb_{0.89}Eu_{0.01}BO_3$ (100% V) (Fig 4, *d, e*). At the same time, in samples $Tb_{0.99}Eu_{0.01}BO_3$ (100% V) faceted microcrystals of the size $6-10\,\mu$m are observed, which contain a large amount of discontinuities of continuity (fig. 4, *f*).

Thus, in the aragonite-structured samples $La_{0.99-x}Tb_xEu_{0.01}BO_3$, as in the compounds $La_{0.98-x}Y_xEu_{0.02}BO_3$ [43], microcrystals of size $1-3\,\mu$m are observed. At the same time, the morphology of microcrystals of these compounds differs significantly at $0.2 < x < 0.99$. In samples $La_{0.99-x}Y_xEu_{0.01}BO_3$ for $x > 0.1$ with an increase in the amount of vaterite, the number of small crystals increases. In compounds $La_{0.1}Y_{0.89}Eu_{0.01}BO_3$ (100% V) microcrystals with a size of $0.3-0.7\,\mu$m are mainly observed. At the same time, in the samples $La_{0.99-x}Tb_xEu_{0.01}BO_3$ with an increase in the amount of the vaterite phase with an increase in the concentration of terbium, uncut microcrystals with significant discontinuity violations are observed, the size of which $\sim 2-10\,\mu$m practically does not change at $0.2 < x < 0.99$.

5. Results of IR spectroscopy

Fig. 5 shows the IR spectra of the samples of the studied $La_{0.99-x}Tb_xEu_{0.01}BO_3$ compounds at $0 \le x \le 0.99$ in the frequency range of B−O bond oscillations. Absorption bands 593, 613, 723, 789, 940 and 1306 cm^{-1} are observed in the spectrum of the sample composition $La_{0.99}Eu_{0.01}BO_3$ (Fig. 5, spectrum *1*). According to the data of X-ray phase analysis, the $La_{0.99}Eu_{0.01}BO_3$ obtained under the conditions of our synthesis crystallizes in the aragonite lattice (Table 1). In the structure of aragonite, each

Table 1. The content of the phases of aragonite (A) and vaterite (V) in orthoborates $La_{1-x-y}Tb_xEu_yBO_3$

Concentration *Re*, at.%			A, %	V_A, Å	V, %	V_V, Å
La	Tb	Eu				
99	0	1	100	123.59	0	–
96.5	2.5	1	100	123.31	0	–
94	5	1	100	123.01	0	–
90	9	1	100	122.61	0	–
79	20	1	100	121.24	0	–
64	35	1	91	120.53	9	114.11
57	42	1	69	120.56	31	114.28
49	50	1	55	120.48	45	114.30
24	75	1	16	120.53	84	114.30
10	89	1	0	–	100	113.18
0	99	1	0	–	100	111.80
0	98	2	0	–	100	112.01
0	96.5	3.5	0	–	100	112.00
0	95	5	0	–	100	112.01
0	90	10	0	–	100	112.14

Note. V_A — is the volume of an aragonite unit cell reduced to $Z = 2$; V_V — volume of the vaterite unit cell, $Z = 2$.

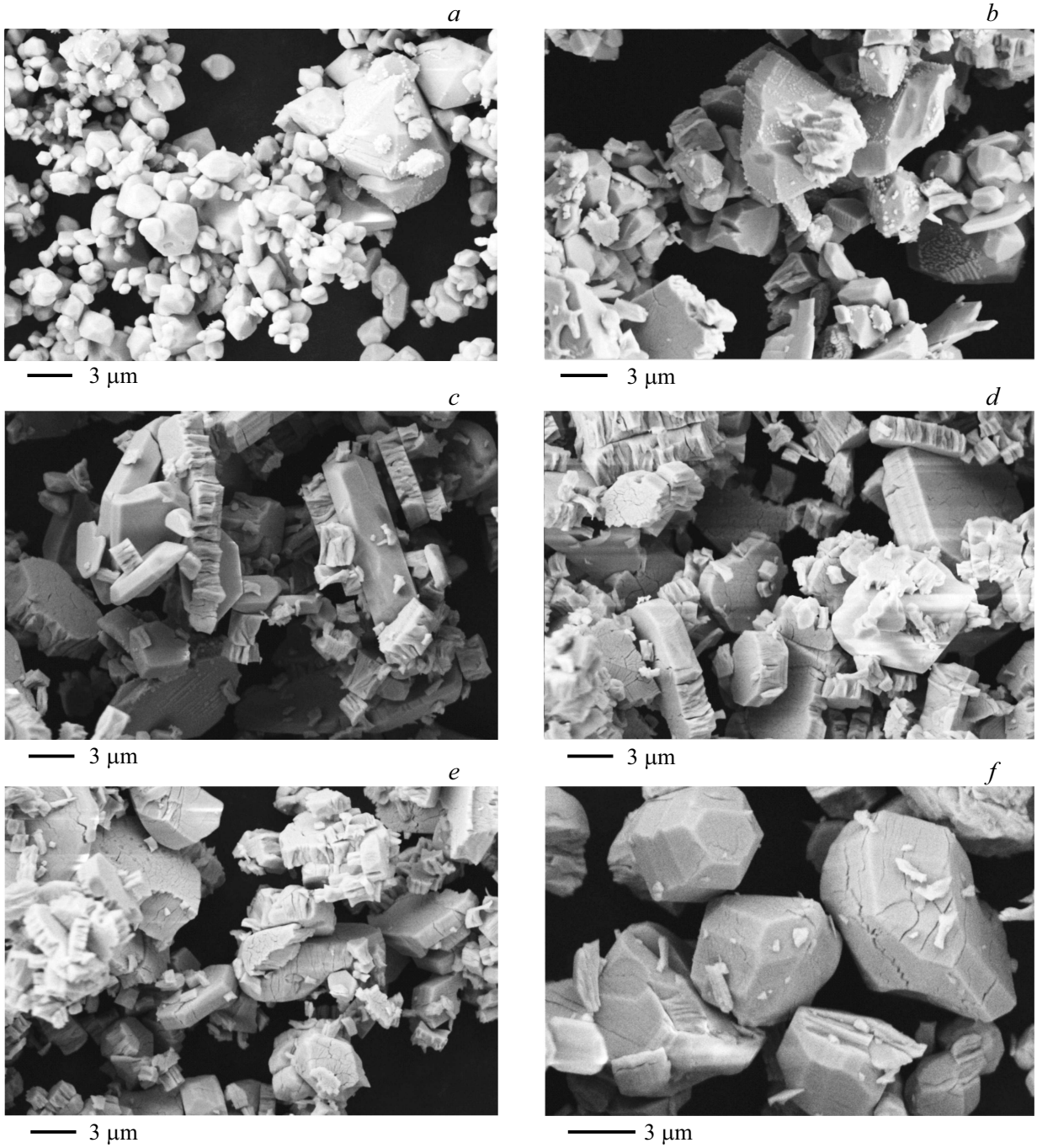

Figure 4. Morphology of orthoborates $La_{0.99-x}Tb_xEu_{0.01}BO_3$ *a* — $La_{0.9}Tb_{0.09}Eu_{0.01}BO_3$; *b* — $La_{0.64}Tb_{0.35}Eu_{0.01}BO_3$; *c* — $La_{0.49}Tb_{0.5}Eu_{0.01}BO_3$; *d* — $La_{0.24}Tb_{0.75}Eu_{0.01}BO_3$; *e* — $La_{0.1}Tb_{0.89}Eu_{0.01}BO_3$; *f* — $Tb_{0.99}Eu_{0.01}BO_3$.

boron atom is surrounded by three oxygen atoms and forms a planar ion $(BO_3)^{3-}$. In accordance with the analysis of internal vibrations of this ion in the structure of aragonite [45], the IR absorption bands 593 and 613 cm^{-1} can be attributed to the in-plane bending vibration ν_4, 723, 789 — to the out-of-plane bending vibration ν_2, and the absorption bands 940 and 1306 cm^{-1} — to symmetric ν_1 and asymmetric ν_3 to stretching vibrations, respectively (Fig. 5, spectrum *1*).

Comparison of the IR spectrum of the compound $La_{0.99}Eu_{0.01}BO_3$ (Fig. 5, spectrum *1*) with the literature data for $LaBO_3$, presented in [41,45,46], shows that the absorption bands we observe are characteristic of the aragonite structure. For compounds of the compositions $La_{0.9}Tb_{0.09}Eu_{0.01}BO_3$ and $La_{0.79}Tb_{0.2}Eu_{0.01}BO_3$ (Fig. 5, spectra *2, 3*), which also have the structure of aragonite (Table 1), the IR spectra are the same as for the orthoborate $La_{0.99}Eu_{0.01}BO_3$. With a further increase in

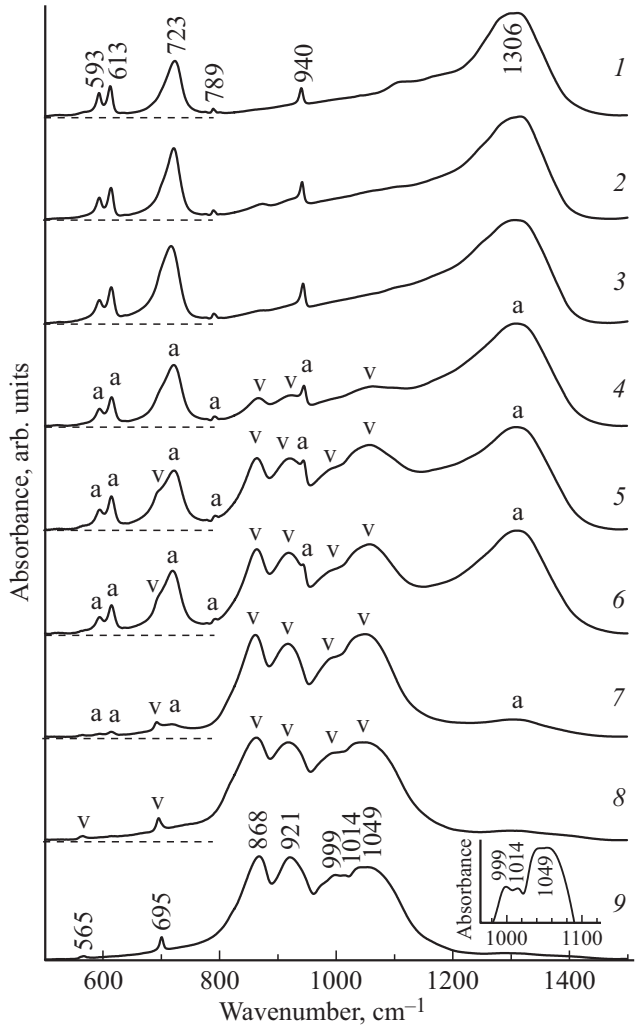

Figure 5. IR spectra of $La_{0.99-x}Tb_xEu_{0.01}BO_3$ orthobotates: *1* — $La_{0.99}Eu_{0.01}BO_3$; *2* — $La_{0.9}Tb_{0.09}Eu_{0.01}BO_3$; *3* — $La_{0.79}Tb_{0.2}Eu_{0.01}BO_3$; *4* — $La_{0.64}Tb_{0.35}Eu_{0.01}BO_3$; *5* — $La_{0.57}Tb_{0.42}Eu_{0.01}BO_3$; *6* — $La_{0.49}Tb_{0.5}Eu_{0.01}BO_3$; *7* — $La_{0.24}Tb_{0.75}Eu_{0.01}BO_3$; *8* — $La_{0.1}Tb_{0.89}Eu_{0.01}BO_3$; *9* — $Tb_{0.99}Eu_{0.01}BO_3$. For the spectra *1*–*8*, the zero values of the ordinate axes are shown by a thin dotted line. In the insert, the spectrum *9* is shown in the range 980–1100 cm^{-1} in enlarged scales along the abscissa and ordinate axes.

the concentration of ions Tb^{3+} in the spectra of samples $La_{0.99-x}Tb_xEu_{0.01}BO_3$ in the range $0.2 < x \leq 0.75$ appear additional bands designated „v". According to the results of X-ray phase analysis, these samples are two-phase and contain phases of aragonite and vaterite (Table 1). In the spectrum of the composition $La_{0.64}Tb_{0.35}Eu_{0.01}BO_3$, the intensity of the bands „v" is insignificant compared to the bands of the aragonite phase „a". The sample contains 92% of the aragonite phase and 8% of the vaterite phase. With an increase of Tb^{3+} ion concentration, intensity of the IR absorption bands, typical for the aragonite phase „a", decreases, while that of the bands, corresponding to the vaterite structure „v", increases (Fig. 5, spectra *4*–*7*). Samples of compositions $La_{0.1}Tb_{0.89}Eu_{0.01}BO_3$ and $Tb_{0.99}Eu_{0.01}BO_3$ according to X-ray phase analysis are single-phase with a vaterite structure. In the vaterite structure, boron atoms have a tetrahedral environment, in contrast to the trigonal environment in the aragonite structure. This is manifested in the IR spectra of these structures. The frequency of stretching vibrations of B–O bonds in the group BO_n (n-coordination number) increases when the coordination number decreases [47]. If in the structure of aragonite the maximum of the absorption band due to stretching vibrations of B–O bonds is near 1300 cm^{-1}, then in the structure of vaterite this absorption is in the range 800–1200 cm^{-1} [47]. In IR spectra of samples $La_{0.1}Tb_{0.89}Eu_{0.01}BO_3$ and $Tb_{0.99}Eu_{0.01}BO_3$ absorption bands are indeed observed within this range: 868, 921, 999, 1014 and 1049 cm^{-1} (Fig. 5, spectra *8, 9*). Similar IR spectra of $TbBO_3$ samples were observed earlier in [41,48] and were characterized by the vaterite structure. It should be noted that the spectrum of the sample $Tb_{0.99}Eu_{0.01}BO_3$ (Fig. 5, spectrum *9*) includes a large set of absorption bands — 565, 695, 868, 921, 999, 1014 and 1049 cm^{-1}, among which the weak band 565 cm^{-1} and a pair of close bands 999 cm^{-1} and 1014 cm^{-1} are not present either in the work [41], or in [48].

Thus, a correspondence has been established between structural modifications and IR absorption spectra of orthoborates $La_{0.99-x}Tb_xEu_{0.01}BO_3$ in the range $0 \leq x \leq 0.99$. At $0 \leq x \leq 0.2$ bands characteristic of the aragonite structure are observed in the IR spectra of these compounds. At $0.2 < x \leq 0.75$ the IR spectra contain bands corresponding to the structures of aragonite and vaterite. At $0.75 < x \leq 0.99$ bands characteristic of the vaterite phase are observed in the IR spectra.

6. Luminescence spectra and luminescence excitation spectra

Fig. 6, *a*, spectrum *1* shows the luminescence excitation spectrum (LES) of the most intense luminescence band of ions Tb^{3+} ($\lambda_{max} = 541.7$ nm) of orthoborate $La_{0.91}Tb_{0.09}BO_3$ having, according to X-ray phase analysis, the structure of aragonite (Table 1). The LES of this sample in the ultraviolet area of the spectrum contains bands with $\lambda_{ex} \sim 231$, 271 and 285 nm ($4f^8 \rightarrow 4f^75d^1$). In addition, resonant bands of ions Tb^{3+} are observed in the wavelength range 300–500 nm, the most intense of which are at $\lambda_{ex} \sim 304$ nm ($^7F_6 \rightarrow {}^5H_6$), 319 nm ($^7F_6 \rightarrow {}^5D_0$), 352 nm ($^7F_6 \rightarrow {}^5D_2$), 360 nm ($^7F_6 \rightarrow {}^5L_{10}$), 371.5 nm ($^7F_6 \rightarrow {}^5G_6$), and 379 nm ($^7F_6 \rightarrow {}^5D_3$), as well as a separately located band 488.5 nm ($^7F_6 \rightarrow {}^5D_4$). It should be noted that the same resonant bands were observed in the LES of orthoborates $LaBO_3$(Tb) at a concentration of ions Tb^{3+} = 2.5, 5, 7.5 and 10 mol.% [41]. In the luminescence excitation spectrum of the most intense luminescence band of ions Tb^{3+} ($\lambda_{max} = 542$ nm) samples $LaBO_3$(5% Tb)

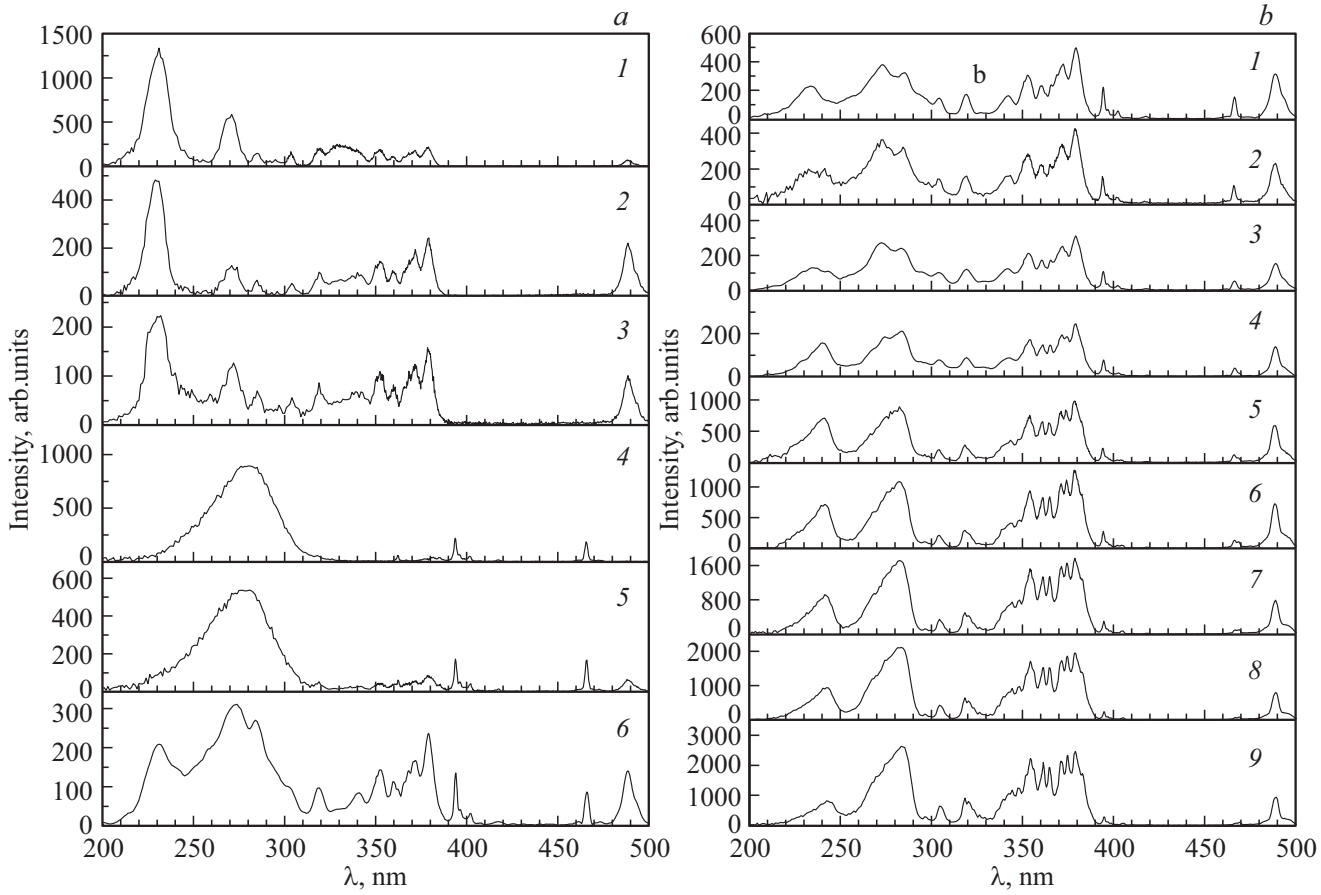

Figure 6. Luminescence excitation spectra of orthoborates. *a*) *1* — $La_{0.91}Tb_{0.09}BO_3$; *2* — $La_{0.9}Tb_{0.09}Eu_{0.01}BO_3$; *3* — $La_{0.79}Tb_{0.2}Eu_{0.01}BO_3$; *4* — $La_{0.99}Eu_{0.01}BO_3$; *5* — $La_{0.9}Tb_{0.09}Eu_{0.01}BO_3$; *6* — $La_{0.79}Tb_{0.2}Eu_{0.01}BO_3$. *1, 2, 3* — $\lambda_{max} = 541.7$ nm; *4, 5, 6* — $\lambda_{max} = 614.5$nm; *b*) *1* — $La_{0.64}Tb_{0.35}Eu_{0.01}BO_3$; *2* — $La_{0.57}Tb_{0.42}Eu_{0.01}BO_3$; *3* — $La_{0.49}Tb_{0.5}Eu_{0.01}BO_3$; *4* — $La_{0.64}Tb_{0.35}Eu_{0.01}BO_3$; *5* — $La_{0.57}Tb_{0.42}Eu_{0.01}BO_3$; *6* — $La_{0.49}Tb_{0.5}Eu_{0.01}BO_3$; *7* — $La_{0.24}Tb_{0.75}Eu_{0.01}BO_3$; *8* — $La_{0.1}Tb_{0.89}Eu_{0.01}BO_3$; *9* — $Tb_{0.99}Eu_{0.01}BO_3$; *1, 2, 3* — $\lambda_{max} = 614.5$ nm; *4, 5, 6, 7, 8, 9* — $\lambda_{max} = 592.5$ nm.

bands 233, 274 and ~ 288 nm were previously observed in the ultraviolet area of the spectrum [49,50].

Based on a comparison of the excitation spectra of luminescence of ions Tb^{3+}, which are found in orthoborates having the structures of vaterite, calcite and aragonite, it can be concluded that the spectral composition of the luminescence of $LaBO_3(Tb)$, having the structure of aragonite, is closer to the spectral the composition of LES compounds $ReBO_3(Tb)$, where Re = Lu, Gd, Eu, Y, having a vaterite structure, than to orthoborates, which have a calcite structure. Indeed, in the LES of ions Tb^{3+} located in orthoborates with the structure of vaterite and aragonite, a number of bands are observed in the wavelength range 300–400 nm, the most intense of which is at 378–379 nm, as well as the band 488–489 nm. While the LES of ions Tb^{3+} in the calcite structure contains only a band with $\lambda_{ex} = 378.5$ nm [4,8–10].

In the luminescence spectrum of orthoborate $LaBO_3(Tb)$, under resonant excitation of ions Tb^{3+} ($\lambda_{ex} = 378$ nm) the emission is observed in the wavelength range of 480–500 nm ($^5D_4 \rightarrow {}^7F_6$), 535–560 nm ($^5D_4 \rightarrow {}^7F_5$), 575–600 nm ($^5D_4 \rightarrow {}^7F_4$) and 615–630 nm ($^5D_4 \rightarrow {}^7F_3$) [41]. A similar luminescence spectrum is observed when the sample $LaBO_3(Tb)$ is excited by light with $\lambda_{ex} = 233$ nm [49,50]. The luminescence intensity in the range of 535–560 nm is several times higher than the luminescence intensity in other ranges of the spectrum.

The luminescence spectrum of the orthoborate $La_{0.91}Tb_{0.09}BO_3$ in the wavelength range 535–635 nm with resonant excitation of ions Tb^{3+} ($\lambda_{ex} = 378.5$ nm) is shown in Fig. 7, spectrum *1*. A similar spectrum is observed at $\lambda_{ex} \sim 231$ nm. The insert to the spectrum *1* shows the decomposition of LS in the range of 535–560 nm into components. The luminescence spectrum of the compound $La_{0.91}Tb_{0.09}BO_3$ contains bands whose maxima are at $\lambda_{max} \sim 540.1$; 541.7; 543.3; 545.1; 546.7; 549.1; 551.3 and 554.7 nm ($^5D_4 \rightarrow {}^7F_5$). The band with $\lambda_{max} = 541.7$ nm has the greatest intensity. At the same time, in the luminescence spectrum of $La_{0.95}Tb_{0.05}BO_3$ samples with the structure of aragonite studied in [49.50], in the wavelength range of 530–560 nm is observed only one band with $\lambda_{max} = 542$ nm, and in the work [41] in $LaBO_3(Tb)$

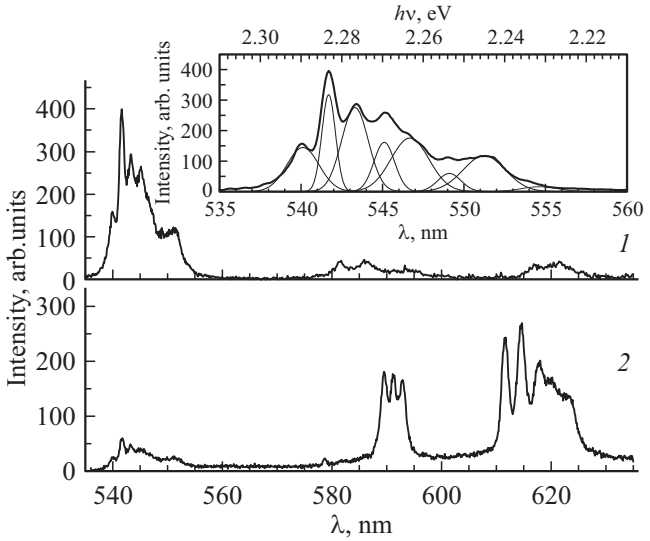

Figure 7. Luminescence spectra of orthoborates. *1* — $La_{0.91}Tb_{0.09}BO_3$; *2* — $La_{0.86}Tb_{0.09}Eu_{0.05}BO_3$. *1, 2* — $\lambda_{ex} = 378.5$ nm. In the insert: decomposition of the spectrum into components. When the spectrum was decomposed, a linear energy scale was used, after the spectrum was decomposed, the transition from eV to nm was carried out.

samples with an aragonite structure in the LS, a band with $\lambda_{max} = 543$ nm is observed, on the long-wave decline of which two shoulders are visible. Such difference in the LS, obtained in this work and in [41,49,50], is most likely due to the insufficiently high spectral resolution, used in the registration of LS in these works.

It is important to note that the spectral composition of the luminescence $LaBO_3$(Tb), having the structure of aragonite, like LES, is closer to the spectral composition of the luminescence of compounds $ReBO_3$(Tb) having the structure of vaterite than to orthoborates having the structure of calcite. In the luminescence spectra of ions Tb^{3+} located in orthoborates having the structure of aragonite and vaterite, in the wavelength range of 530−560 nm, a number of bands are observed, but one band has the greatest intensity, while in orthoborates with the structure of calcite in this spectral range two bands of the same intensity are observed.

6.1. Luminescence excitation spectra

In the excitation spectrum of the most intense luminescence band of Eu^{3+} ions orthoborate $La_{0.99}Eu_{0.01}BO_3$ ($\lambda_{max} = 614.5$ nm ($^5D_0 \rightarrow {}^7F_2$)) having the structure of aragonite (Table 1), a wide band is observed in the ultraviolet area of the spectrum ($\lambda = 230-330$ nm) with a maximum at ~ 280 nm (charge transfer band — CTB) (Fig. 6, *a*, spectrum *4*). LES of $La_{0.99}Eu_{0.01}BO_3$ also contains several narrow bands in a wavelength range of 290−500 nm, corresponding to resonance excitation of ions Eu^{3+}. The bands with maxima at $\lambda_{ex} = 394$ nm ($^7F_0 \rightarrow {}^5L_6$) and 465.5 nm ($^7F_0 \rightarrow {}^5D_2$) are the most intense in the long-wavelength area of the spectrum (fig. 6, *a*, spectrum *4*).

Luminescence excitation spectrum (LES) of the most intense band of the ions Eu^{3+} of orthoborate $La_{0.9}Tb_{0.09}Eu_{0.01}BO_3$ ($\lambda_{max} = 614.5$ nm ($^5D_0 \rightarrow {}^7F_2$)), having the structure of aragonite (Table 1), is shown in Fig. 6, *a*, spectrum *5*. In LES of this sample, as in the orthoborate $La_{0.99}Eu_{0.01}BO_3$, the most intense is the wide short-wave band ($\lambda = 230-340$ nm) with a maximum at $\lambda_{ex} \sim 280$ nm (charge transfer band — CTB). In LES there can be seen bands corresponding to the resonant excitation of ions Eu^{3+} ($\lambda_{ex} = 394$ and 466 nm), a number of narrow bands in the wavelength range 360−390 nm, band 378.5 and 488.5 nm. It should be noted that bands 378.5 and 488.5 nm, as well as narrow bands in the wavelength range 340−390 nm are observed in the excitation spectra of ions Tb^{3+} in samples $La_{0.91}Tb_{0.09}BO_3$ and $La_{0.9}Tb_{0.09}Eu_{0.01}BO_3$ (Fig. 6, *a*, spectra *1, 2*). With an increase in the concentration of terbium in the luminescence excitation spectra of the most intense luminescence bands of ions Eu^{3+} orthoborates $La_{0.99-x}Tb_xEu_{0.01}BO_3$, there are noticeable changes. In LES of ions Eu^{3+} in the compound $La_{0.79}Tb_{0.2}Eu_{0.01}BO_3$ having the structure of aragonite (Table 1), three bands with maxima at $\lambda_{ex} = 231$, 272 and 285 nm are observed in the short-wavelength area of the spectrum, the intensities of narrow bands in the range 300−370 nm, as well as bands 378.5 and 488.5 nm are amplified. Resonant excitation bands of ions Eu^{3+} 394 and 466 nm are also observed (Fig. 6, *a*, spectrum *6*). It should be noted that bands 231, 272 and 285 nm, narrow bands in the range of 310−370 nm, as well as bands 378.5 and 488.5 nm in the LES of ions Eu^{3+} are observed in the LES of ions Tb^{3+} in the samples $La_{0.79}Tb_{0.2}Eu_{0.01}BO_3$ (Fig. 6, *a*, spectrum *3*). Thus, when ions Tb^{3+} are excited, the luminescence of ions Eu^{3+} is observed, which clearly indicates the transfer of energy from ions Tb^{3+} to Eu^{3+}.

Excitation spectra of the luminescence of ions Eu^{3+} ($\lambda_{max} = 614.5$ nm) corresponding to the aragonite modification of $La_{0.99-x}Tb_xEu_{0.01}BO_3$, with $x = 0.35$, 0.42 and 0.5, containing 91, 69 and 55% aragonite, respectively (Table 1), are shown in Fig. 6, *b*, spectra *1, 2, 3*. The spectra of these samples show the same bands as in the sample $La_{0.79}Tb_{0.2}Eu_{0.01}BO_3$ (Fig. 6, *a*, spectrum *6*), which has the structure of aragonite. At the same time, in the excitation spectra of the luminescence of ions Eu^{3+} ($\lambda_{max} = 692.5$ nm) corresponding to the luminescence of ions Eu^{3+} in the vaterite modification of $La_{0.99-x}Tb_xEu_{0.01}BO_3$ orthoborates in samples $La_{0.99-x}Tb_xEu_{0.01}BO_3$ ($x = 0.35$, 0.42 and 0.5) in the short-wavelength area of the spectrum, the two bands with $\lambda_{ex} \sim 241$ and 283 nm are the most intense, as in the LES of ions Tb^{3+} in the vaterite modification $LuBO_3$(Tb). A series of narrow bands in the range 300−380 nm, bands 378.5 and 488.5 nm, corresponding to the excitation of the luminescence of ions Tb^{3+} in the vaterite modification $LuBO_3$(Tb), is also observed in the LES of these samples. In addition, in these samples, along with the resonant excitation bands of the ions $Eu^{3+} \sim 394$ and 466 nm characteristic of the aragonite

structure, the 469 nm band appears (Fig. 6, *b*, spectra *4, 5, 6*; fig. 8, spectra *5, 6*). LES of ions Eu^{3+} ($\lambda_{max} = 592.5$ nm) in samples $La_{0.99-x}Tb_xEu_{0.01}BO_3$ ($x = 0.75$, 0.89 and 0.99) containing 84, 100 and 100% vaterite, respectively (Table 1), are represented in (Fig. 6, *b*, spectra *7, 8, 9*). The spectra of these samples show the same bands as in the compound $La_{0.49}Tb_{0.5}Eu_{0.01}BO_3$ (Fig. 6, *b*, spectrum *6*). It should be noted that the luminescence intensity of ions Eu^{3+} (I_{Eu}) when excited in the excitation bands of ions Tb^{3+} ($\lambda_{ex} = 283$, 378.5 nm) increases with increasing concentration of ions Tb^{3+}, while I_{Eu} under resonant excitation ($\lambda_{ex} = 394$ nm) changes slightly. In samples $Tb_{0.99}Eu_{0.01}BO_3$ the luminescence intensity of ions Eu^{3+} when excited by light with $\lambda_{ex} = 283$ and 378.5 nm is practically an order of magnitude higher than when $\lambda_{ex} = 394$ nm. Thus, in samples $La_{0.99-x}Tb_xEu_{0.01}BO_3$ having the structure of vaterite, as well as in compounds with the structure of aragonite, when excited by ions Tb^{3+} the luminescence of Eu^{3+} ions is observed, which clearly indicates the transfer of energy from ions Tb^{3+} to Eu^{3+}.

Fig. 8 shows the luminescence excitation spectra (LES) of ions Eu^{3+} in samples $La_{0.99-x}Tb_xEu_{0.01}BO_3$ ($0 \le x \le 0.99$) in the spectral range 462–472 nm. In the LES of ions Eu^{3+} orthoborate $La_{0.99}Eu_{0.01}BO_3$ ($\lambda_{max} = 614.5$ nm ($^5D_0 \rightarrow {}^7F_2$)), having the structure of aragonite (Table 1), in the area of 462–472 nm, there is one band with a maximum at ~ 466 nm (Fig. 8, spectrum *1*). The same spectrum is observed in samples $La_{0.9}Tb_{0.09}Eu_{0.01}BO_3$ and $La_{0.79}Tb_{0.2}Eu_{0.01}BO_3$, which also have the structure of aragonite (Table 1, Fig. 8, spectrum *2*). In the excitation spectra of the ions Eu^{3+} characteristic of the aragonite structure ($\lambda_{max} = 614.5$ nm), in compounds $La_{0.64}Tb_{0.35}Eu_{0.01}BO_3$; $La_{0.57}Tb_{0.42}Eu_{0.01}BO_3$; $La_{0.49}Tb_{0.5}Eu_{0.01}BO_3$ containing 91% aragonite (A) and 9% vaterite (V); 72% A and 28% V; 55% A and 45% V respectively, (table 1), only the band ~ 466 nm is also observed (Fig. 8, spectra *3, 4*). At the same time, in these samples for the excitation spectra of the luminescence of ions Eu^{3+} characteristic of the vaterite modification ($\lambda_{max} = 625.5$ and 592.5 nm), two bands with $\lambda_{max} \sim 466$ and 469 nm are observed (Fig. 8, spectra *5, 6*). It should be noted that the 469 nm band is clearly visible even in the LES of a sample containing only 9% vaterite (Fig. 8, spectrum *5*). In samples $La_{0.99-x}Tb_xEu_{0.01}BO_3$ ($0.89 \le x \le 0.99$) having a vaterite structure, two bands ~ 466 and 469 nm are observed (fig. 8, spectrum *8*).

Thus, in the excitation spectra of luminescence of ions Eu^{3+} in orthoborates $La_{0.99-x}Tb_xEu_{0.01}BO_3$ having a vaterite structure, as in $La_{0.99-x}Y_xEu_{0.01}BO_3$ compounds [43], there is a band with $\lambda_{max} = 469$ nm, while as in these compounds having the structure of aragonite, this band is absent. Therefore, the presence or absence in the LES of a band with $\lambda_{ex} = 469$ nm can serve as an indicator of the structural state of orthoborates $La_{0.99-x}Re_xEu_{0.01}BO_3$, $Re = Y, Tb$.

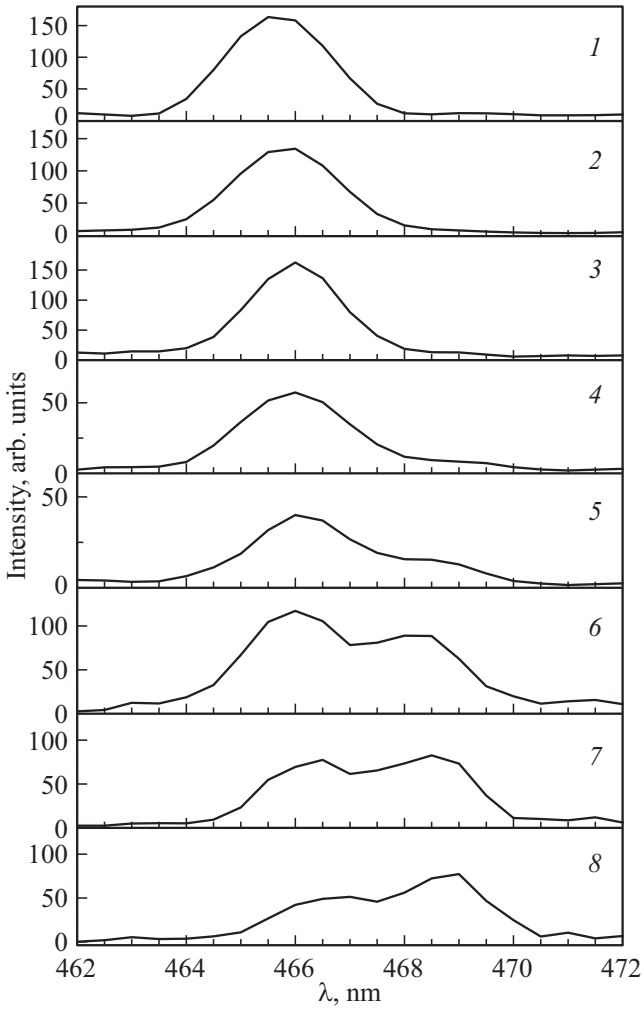

Figure 8. Excitation spectra of luminescence of orthoborates $La_{0.99-x}Tb_xEu_{0.01}BO_3$, in the wavelength range 462–472 nm. *1* — $La_{0.99}Eu_{0.01}BO_3$; *2* — $La_{0.9}Tb_{0.09}Eu_{0.01}BO_3$; *3* — $La_{0.64}Tb_{0.35}Eu_{0.01}BO_3$; *4* — $La_{0.49}Tb_{0.5}Eu_{0.01}BO_3$; *5* — $La_{0.64}Tb_{0.35}Eu_{0.01}BO_3$; *6* — $La_{0.49}Tb_{0.5}Eu_{0.01}BO_3$; *7* — $La_{0.24}Tb_{0.75}Eu_{0.01}BO_3$; *8* — $Tb_{0.99}Eu_{0.01}BO_3$. *1, 2, 3, 4* — $\lambda_{max} = 614.5$ nm; *5* — $\lambda_{max} = 625.5$ nm; *6, 7, 8* — 592.5 nm.

6.2. Luminescence spectra

When the luminescence of ions Eu^{3+} is excited in orthoborates $ReBO_3(Eu)$, where Re = Lu, La, Tb, Eu, Gd, Y by light corresponding to the area of intense absorption of the sample, for example, when excitation in the charge transfer band (CTB) ($\lambda_{ex} = 230$–290 nm), it is possible to obtain information about the local environment of the sample in the near-surface layer of the crystal. With resonance excitation of the luminescence of Eu^{3+} ions in the crystal transparency area ($\lambda_{ex} \sim 394$ and ~ 466 nm), we obtain information about the immediate environment of Eu^{3+} ions in the crystal volume [9,10]. Fig. 9 shows the luminescence spectra (LS) of ions Eu^{3+} in orthoborates $La_{0.99-x}Tb_xEu_{0.01}BO_3$ ($0 \le x \le 0.99$) in the spectral range of 575–635 nm when excited by light in the area of intense absorption of the

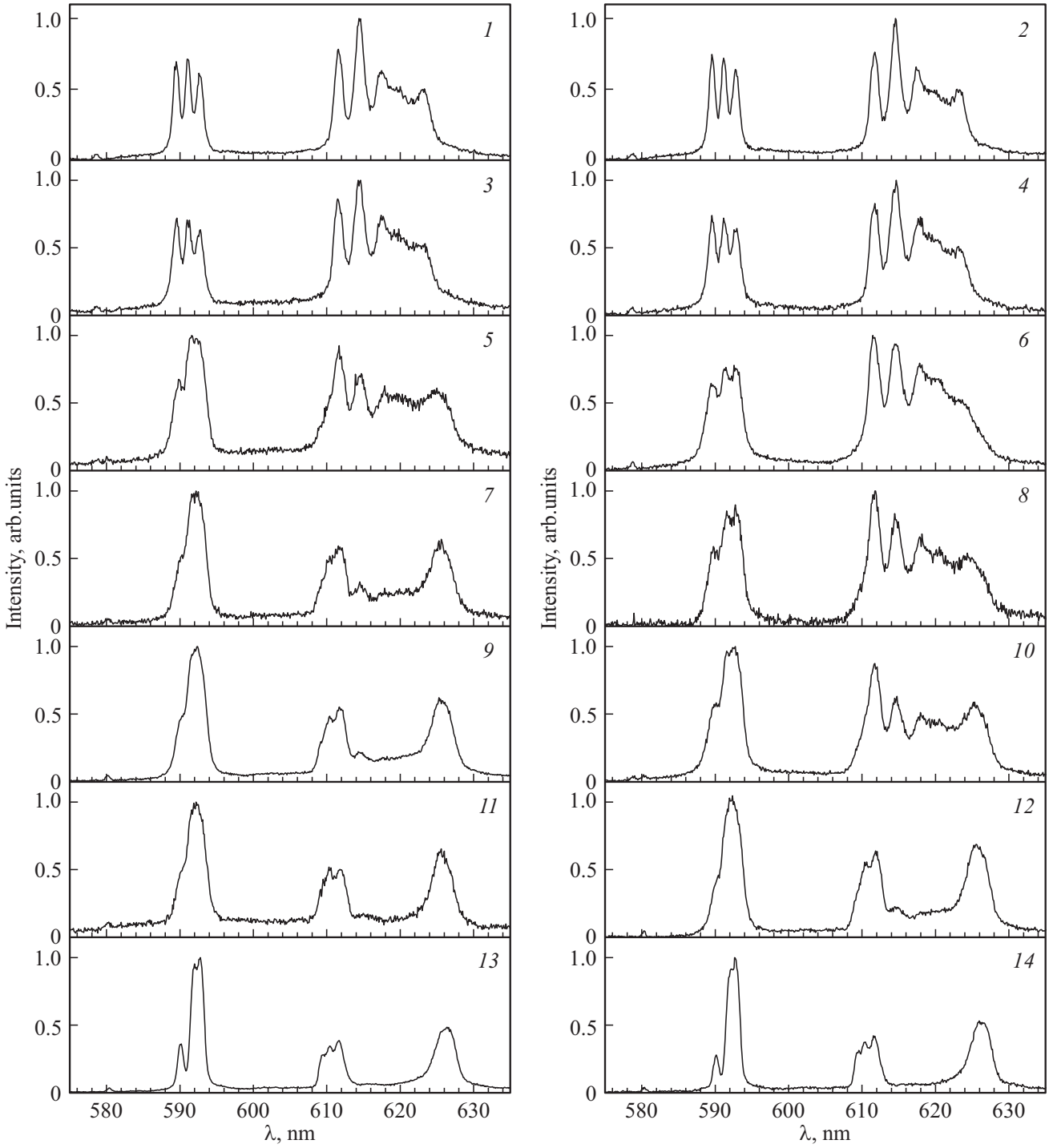

Figure 9. Luminescence spectra of orthoborates. $La_{0.99-x}Tb_xEu_{0.01}BO_3$ *1, 2* — $La_{0.99}Eu_{0.01}BO_3$; *3, 4* — $La_{0.9}Tb_{0.09}Eu_{0.01}BO_3$; *5, 6* — $La_{0.64}Tb_{0.35}Eu_{0.01}BO_3$; *7, 8* — $La_{0.57}Tb_{0.42}Eu_{0.01}BO_3$; *9, 10* — $La_{0.49}Tb_{0.5}Eu_{0.01}BO_3$; *11, 12* — $La_{0.24}Tb_{0.75}Eu_{0.01}BO_3$; *13, 14* — $Tb_{0.99}Eu_{0.01}BO_3$. *1, 3, 5, 7, 9, 11, 13* — $\lambda_{ex} = 283$ nm; *2, 4, 6, 8, 10, 12, 14* — $\lambda_{ex} = 394$ nm

sample ($\lambda_{ex} \sim 230-290$ nm) and with resonant excitation of ions Eu^{3+} ($\lambda_{ex} = 394$ nm). Luminescence spectra of these samples having at $0 \le x \le 0.2$ the structure of aragonite (Table 1), are identical. Fig. 9, spectra *1–4* shows the LS of compounds $La_{0.99}Eu_{0.01}BO_3$ and $La_{0.9}Tb_{0.09}Eu_{0.01}BO_3$. The luminescence spectra of the near-surface layer and the volume of these samples coincide. They contain the same as in the samples $La_{0.98}Eu_{0.02}BO_3$ [38], bands with $\lambda_{max} = 578.6$ nm ($^5D_0 \rightarrow {}^7F_0$), 589.4, 591 and 592.6 nm ($^5D_0 \rightarrow {}^7F_1$), and band 611.6, 614.5, 617.4, 619.8 and 623 nm ($^5D_0 \rightarrow {}^7F_2$). With an increase in the concentration of ions Tb^{3+}, changes occur simultaneously in the lumines-

cence spectra of both the near-surface layer and the volume of samples. In the compound $La_{0.64}Tb_{0.35}Eu_{0.01}BO_3$, which contains 91% aragonite (A) and 9% vaterite (V) (Table 1), in the luminescence spectra at $\lambda_{ex} = 283$ and 394 nm, there are changes in the ratios between the band intensities in the wavelength range 588–596 nm (Fig. 9, spectra *5, 6*). In luminescence spectra of the near-surface layer and volume of samples $La_{0.57}Tb_{0.42}Eu_{0.01}BO_3$ and $La_{0.49}Tb_{0.5}Eu_{0.01}BO_3$ containing 69% A, 31% V and 55% A, 45% V, respectively (Table 1), the intensity of the band with $\lambda_{max} \sim 592.5$ nm, corresponding to the vaterite modification $ReBO_3$(Eu), Re = Lu, Tb, Gd increases [3–5,9.10]. In addition, bands with $\lambda_{max} \sim 580.3$ and ~ 626 nm, appear in the LS also characteristic of the vaterite modification $ReBO_3$(Eu) (Fig. 9, spectra *7–10*). In luminescence spectra of the near-surface layer and sample volume $La_{0.24}Tb_{0.75}Eu_{0.01}BO_3$ (16% A and 84% V) (Table 1), mainly bands characteristic of the vaterite modification of $ReBO_3$(Eu) are observed. The fact that this sample contains a small amount of the aragonite phase is evidenced by the presence of a weak band in the LS with $\lambda_{max} = 614.5$ nm (Fig. 9, spectra *11, 12*). In luminescence spectra of orthoborate $Tb_{0.99}Eu_{0.01}BO_3$ having the structure of vaterite, bands characteristic of vaterite modification of orthoborates are observed (Fig. 9, spectra *13, 14*).

Based on the above results, it can be concluded that the formation of the vaterite phase in the microcrystals of the orthoborate $La_{0.99-x}Tb_xEu_{0.01}BO_3$ occurs in the entire sample simultaneously — both in volume, and in the near-surface layer of microcrystals having the structure of aragonite. While in the orthoborates $La_{1-x}Re_xBO_3$(Eu), where Re = Lu, Y, the formation of the vaterite phase occurs first in the volume of microcrystals having the structure of aragonite, and then, with an increase of x also in the near-surface layer of microcrystals [38.43].

It should be noted that, as noted in section 4, there are significant differences in the morphology of these microcrystals. In $La_{0.99-x}Tb_xEu_{0.01}BO_3$ samples, with an increase in the amount of the vaterite phase with an increase in x, uncut microcrystals with significant discontinuity violations are observed, the size of which is $\sim 2-10\,\mu$m practically does not change at $0.2 < x < 0.99$. While in the samples $La_{0.99-x}Y_xEu_{0.01}BO_3$ for $x > 0.1$ with an increase in the amount of vaterite, the number of small microcrystals with a size of $0.3-0.7\,\mu$m increases.

As shown in [41], the maximum luminescence intensity of orthoborates $LaBO_3$(Tb), having an aragonite structure is observed at a concentration of terbium ~ 5 mol.%. With a further increase in the concentration of Tb^{3+}, the luminescence intensity of ions Tb^{3+} (I_{Tb}) decreases as a result of concentration quenching of luminescence.

Fig. 10 shows the luminescence spectra of ions Tb^{3+} and Eu^{3+} in samples $La_{0.99-x}Tb_xEu_{0.01}BO_3$ ($0 \le x \le 0.99$) when excited in the resonant absorption band of ions Tb^{3+} ($\lambda_{ex} = 378.5$ nm ($^7F_6 \rightarrow {}^5D_3$)). The dependences of the integral luminescence intensities of the ions Tb^{3+} (S_{Tb}) and Eu^{3+} (S_{Eu}) in these samples are shown in Fig. 11. S_{Tb}

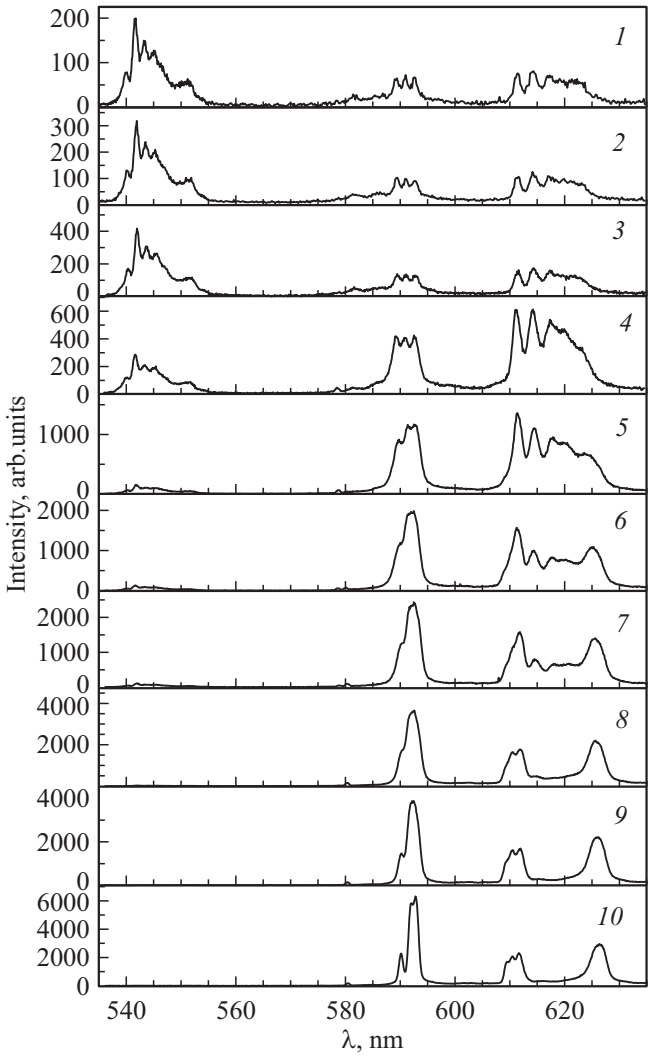

Figure 10. Luminescence spectra of ions Tb^{3+} and Eu^{3+} in orthoborates $La_{0.99-x}Tb_xEu_{0.01}BO_3$ when excited in absorption band Tb^{3+} ($\lambda_{ex} = 378.5$ nm) *1* — $La_{0.965}Tb_{0.025}Eu_{0.01}BO_3$; *2* — $La_{0.94}Tb_{0.05}Eu_{0.01}BO_3$; *3* — $La_{0.9}Tb_{0.09}Eu_{0.01}BO_3$; *4* — $La_{0.79}Tb_{0.2}Eu_{0.01}BO_3$; *5* — $La_{0.64}Tb_{0.35}Eu_{0.01}BO_3$; *6* — $La_{0.57}Tb_{0.42}Eu_{0.01}BO_3$; *7* — $La_{0.49}Tb_{0.5}Eu_{0.01}BO_3$; *8* — $La_{0.24}Tb_{0.75}Eu_{0.01}BO_3$; *9* — $La_{0.1}Tb_{0.89}Eu_{0.01}BO_3$; *10* — $Tb_{0.99}Eu_{0.01}BO_3$.

and S_{Eu} — areas under the luminescence spectra curves of ions Tb^{3+} and Eu^{3+} (Fig. 10) in the ranges of 535–560 nm (2.318–2.214 eV) and 575–635 nm (2.156–1.953 eV), respectively. With an increase in the concentration of Tb^{3+}, the intensity of the luminescence of ions Tb^{3+} initially increases, reaches a maximum at $x \sim 0.09$ (Fig. 10, 11), and then decreases due to the concentration quenching of the luminescence. At $0.89 \le x \le 0.99$, the luminescence intensity of ions Tb^{3+} in $La_{0.99-x}Tb_xEu_{0.01}BO_3$ compounds is close to zero. It should be noted that the luminescence spectrum of ions Tb^{3+} remains almost unchanged at $0 \le x \le 0.75$.

Table 2. Dependence of the integral luminescence intensity of ions Eu^{3+} (S_{Eu}) in orthoborates $Tb_{1-y}Eu_yBO_3$ from the concentration Eu^{3+}

Eu, at.%	1	2	3.5	5	10
S_{Eu}, arb. units	143.7	158.2	148.7	138.1	97.2

At the same time, a completely different change in the luminescence intensity and spectral characteristics is observed for ions Eu^{3+}. Luminescence spectra of ions Eu^{3+} in orthoborates $La_{0.99-x}Tb_xEu_{0.01}BO_3$ having at $0 \le x \le 0.2$ the structure of aragonite (Table 1), in the wavelength range 575–635 nm contain bands characteristic of compounds $La_{0.99}Eu_{0.01}BO_3$, which have the structure of aragonite (Fig. 10, spectra *1–4*). At $x = 0.35$ (91% A, 9% V), 0.42 (69% A, 31% V), 0.5 (55% A, 45% V), there are changes in the intensity ratios bands in LS of ions Eu^{3+} (Fig. 10, spectra *5–7*). For $x = 0.75$ (16% A, 84% V), 0.89 (100% V) and 0.99 (100% V) luminescence spectra of ions Eu^{3+} in compounds $La_{0.99-x}Tb_xEu_{0.01}BO_3$ contain bands characteristic of the vaterite modification of orthoborates $ReBO_3$(Eu), Re = Lu, Tb, Gd (Fig. 10, spectra *8–10*).

The luminescence intensity of ions Eu^{3+} in $La_{0.99-x}Tb_xEu_{0.01}BO_3$ samples when excited in the absorption band of ions Tb^{3+} continuously it grows with increasing concentration of Tb^{3+} (Fig. 10, 11). To determine the concentration of ions Eu^{3+} at which the luminescence intensity of orthoborates $Tb_{1-y}Eu_yBO_3$, when excited in the absorption band of ions Tb^{3+} ($\lambda_{ex} = 378.5$ nm), has a maximum, we have conducted studies of the spectral characteristics of these compounds at concentrations of ions Eu^{3+} 1, 2, 3.5, 5 and 10 at.%. The normalized luminescence spectra of these samples having a vaterite structure (Table 1), coincide and contain bands characteristic of the vaterite modification $ReBO_3$(Eu) (Fig. 10, spectrum *10*). Table 2 shows the integral intensities of the luminescence spectra of Eu^{3+} ions (S_{Eu}). As can be seen from the table, the maximum value of S_{Eu} in the orthoborate $Tb_{1-y}Eu_yBO_3$ is observed at the concentration of ions Eu^{3+} 2 at.%.

It is important to note that in the samples $La_{0.99-x}Tb_xEu_{0.01}BO_3$ at $0.89 \le x \le 0.99$ when excited in the resonance absorption band of ions Tb^{3+} ($\lambda_{ex} = 378.5$ nm), there is practically no luminescence of ions Tb^{3+}, while there is an intense luminescence of ions Eu^{3+}. This is an illustration of the fact that the transfer of electron excitation energy from ions Tb^{3+} to Eu^{3+} does not occur by the process of emission — adsorption of a photon, but as a result of non-radiative energy transfer due to the Coulomb interaction between these ions.

One of the main characteristics of energy transfer from the donor (in our case Tb^{3+}) to the acceptor (Eu^{3+}) is the efficiency of this process (η). The efficiency of energy transfer from the donor to the acceptor can be judged by the decrease in the intensity of the donor luminescence when the acceptor is added to the compound. Comparing the integral luminescence intensities of the donor (Tb^{3+}) in the absence and presence of an acceptor (Eu^{3+}), it is possible to determine the efficiency of the energy transfer process by the formula

$$\eta = (1 - S_{Tb+Eu}/S_{Tb}) \cdot 100\%,$$

where S_{Tb} and S_{Tb+Eu} — integral luminescence intensities of ions Tb^{3+} in compounds $La_{0.91}Tb_{0.09}BO_3$ and $La_{0.86}Tb_{0.09}Eu_{0.05}BO_3$ when excited in the absorption band of ions Tb^{3+} ($\lambda_{ex} = 378.5$ nm). S_{Tb} and S_{Tb+Eu} — areas under the curves of luminescence spectra in the wavelength range 535–560 nm (Fig. 7, spectra *1, 2*). When determining S_{Tb} and S_{Tb+Eu}, the linear energy scale of the abscissa axis in eV was used. The values of S_{Tb} and S_{Tb+Eu} are equal to 11.08 and 1.57 arb. units. The value of $\eta = 86\%$, which indicates the high efficiency of the energy transfer process from the ions Tb^{3+} to Eu^{3+} in the orthoborate $La_{0.86}Tb_{0.09}Eu_{0.05}BO_3$ when excited in the absorption band of ions Tb^{3+} ($\lambda_{ex} = 378.5$ nm). As noted in the introduction, the highest efficiency of energy transfer from Tb^{3+} to $Eu^{3+}\eta = 99\%$ was observed in $Tb(OH)_3 : Eu^{3+}$ samples at Eu^{3+} ion concentration 3 mol.% [24].

Let us discuss in more detail the dependence of the spectral position of the band corresponding to the transition ($^5D_0 \rightarrow {}^7F_0$) in ions Eu^{3+}, from the concentration of ions $Tb^{3+}(x)$ in orthoborates $La_{0.99-x}Tb_xEu_{0.01}BO_3$. As noted, the maxima of this band are in compounds $La_{0.99-x}Y_xEu_{0.01}BO_3$ having structures of aragonite (A) and vaterite (V) are at $\lambda_{max} \sim 578.6$ and ~ 580.4 nm,

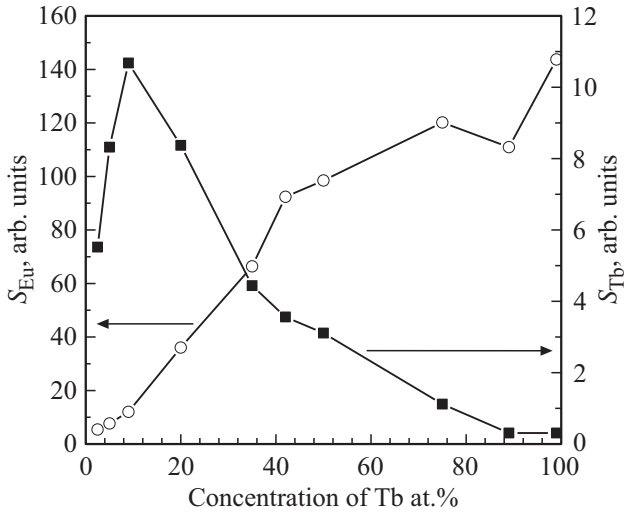

Figure 11. Dependences of integral luminescence intensities of ions Tb^{3+} (S_{Tb}) and Eu^{3+} (S_{Eu}) in orthoborates $La_{0.99-x}Tb_xEu_{0.01}BO_3$, when excited in the Tb^{3+} absorption band ($\lambda_{ex} = 378.5$ nm) Circle — S_{Eu}; square — S_{Tb}; S_{Tb} and S_{Eu} — areas under the curves of the luminescence spectra (Fig. 10) in the wavelength ranges 535–560 nm (2.318–2.214 eV) and 575–635 nm (2.156–1.953 eV), respectively. When determining S_{Tb} and S_{Eu}, the linear energy scale of the abscissa axis in eV was used.

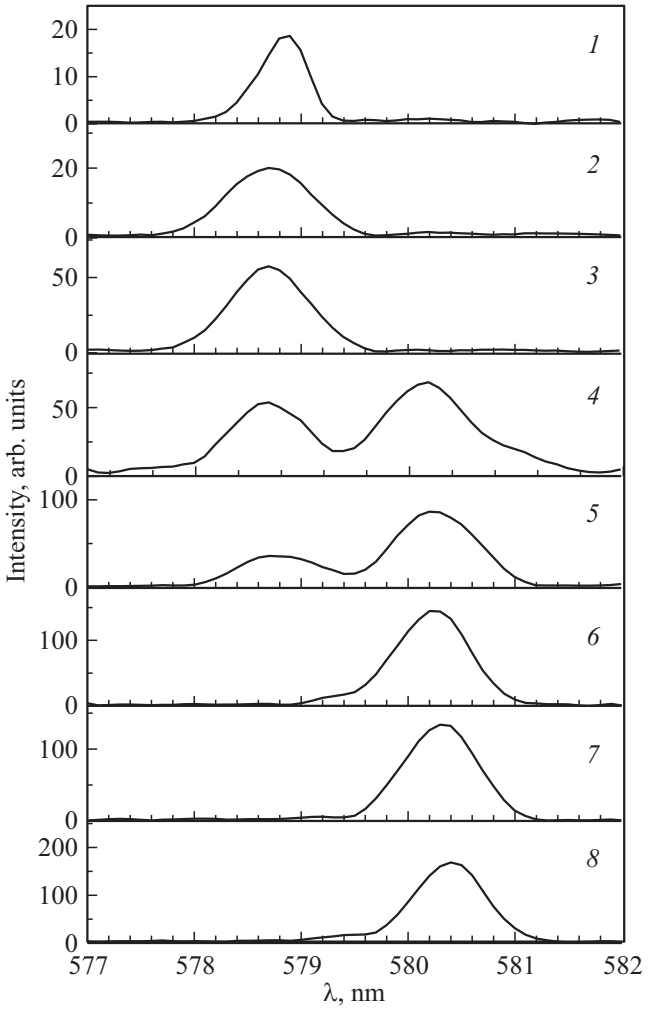

Figure 12. Luminescence spectra of orthoborates. $La_{0.99-x}Tb_xEu_{0.01}BO_3$, in the wavelength range 577–582 nm. *1* — $La_{0.9}Tb_{0.09}Eu_{0.01}BO_3$; *2* — $La_{0.79}Tb_{0.2}Eu_{0.01}BO_3$; *3* — $La_{0.64}Tb_{0.35}Eu_{0.01}BO_3$; *4* — $La_{0.57}Tb_{0.42}Eu_{0.01}BO_3$; *5* — $La_{0.49}Tb_{0.5}Eu_{0.01}BO_3$; *6* — $La_{0.24}Tb_{0.75}Eu_{0.01}BO_3$; *7* — $La_{0.1}Tb_{0.89}Eu_{0.01}BO_3$; *8* — $Tb_{0.99}Eu_{0.01}BO_3$. $\lambda_{ex} = 378.5$ nm.

respectively [43]. Fig. 12 shows the luminescence spectra of samples $La_{0.99-x}Tb_xEu_{0.01}BO_3$ in the spectral range 577–582 nm with resonant excitation of ions Tb^{3+} ($\lambda_{ex} = 378.5$ nm). Similar results were also obtained with resonant excitation of ions Eu^{3+} ($\lambda_{ex} = 394$ nm). In LS samples $La_{0.99-x}Tb_xEu_{0.01}BO_3$ at $x = 0.09$, 0.2 and 0.35 containing 100, 100 and 91% aragonite, respectively (Table 1), a band with $\lambda_{max} \sim 578.6$ nm is observed (Fig. 12, spectra *1–3*).

Special attention should be paid to the luminescence spectra of orthoborates $La_{0.57}Tb_{0.42}Eu_{0.01}BO_3$ (69% A, 31% V) and $La_{0.49}Tb_{0.5}Eu_{0.01}BO_3$ (55% A, 45% V). They contain simultaneously two bands with $\lambda_{max} \sim 578.6$ and ~ 580.3 nm, characteristic of aragonite and vaterite structures, respectively (Fig. 12, spectra *4, 5*). It is important to note that simultaneous registration of two bands characteristic of aragonite and vaterite structures corresponding to the transition ($^5D_0 \rightarrow {}^7F_0$) in ions Eu^{3+}, implemented for the first time. In LS samples $La_{0.24}Tb_{0.75}Eu_{0.01}BO_3$ (16% A, 84% V), $La_{0.1}Tb_{0.89}Eu_{0.01}BO_3$ (100% V) and $Tb_{0.99}Eu_{0.01}BO_3$ (100% V) there is only one band with $\lambda_{max} = 580.3$ and 580.4 nm, respectively (Fig. 12, spectra *6–8*).

Thus, in the luminescence spectra of orthoborates $La_{0.99-x}Tb_xEu_{0.01}BO_3$ the maximum of the band corresponding to the transition ($^5D_0 \rightarrow {}^7F_0$) in ions Eu^{3+}, in samples having the structure of aragonite and vaterite, is at $\lambda_{max} \sim 578.6$ nm and ~ 580.4 nm, respectively. Therefore, the bands corresponding to the transition $^5D_0 \rightarrow {}^7F_0$, can serve as an indicator of the structural state of the sample.

7. Conclusion

In this paper, studies of the structure, morphology, IR spectra, as well as luminescence excitation spectra and luminescence spectra of the near-surface layer and volume synthesized at 970°C microcrystals of orthoborates $La_{0.99-x}Tb_xEu_{0.01}BO_3$ at $0 \le x \le 0.99$ were carried out. An unambiguous correspondence between the structure and spectral characteristics of these compounds was established.

It is shown that in the orthoborates $La_{0.99-x}Tb_xEu_{0.01}BO_3$, the same as in $La_{0.99-x}Y_xEu_{0.01}BO_3$, an increase of x leads to a sequential change in their structural state and spectral characteristics.

– At $0 \le x \le 0.2$ compounds are single-phase and have the structure of aragonite (SG $Pnam$). The luminescence spectra of ions Eu^{3+} corresponding to the aragonite structure contain, as in $La_{1-x}Re_xBO_3(Eu)$ compounds, where Re = Lu, Y, bands, with $\lambda_{max} = 589.4$, 591 and 592.6 nm, corresponding to the transition $^5D_0 \rightarrow {}^7F_1$, as well as the band 611.6, 614.5, 617.4, 619.8 and 623 nm ($^5D_0 \rightarrow {}^7F_2$). In the luminescence excitation spectrum of ions Eu^{3+}, along with the bands observed in $La_{1-x}Re_xBO_3(Eu)$ samples, where Re = Lu, Y, bands appear, corresponding to the excitation of the luminescence of ions Tb^{3+}. The IR spectra contain the absorption bands of 593, 613, 723, 789, 940 and 1306 cm^{-1} which are typical for the aragonite phase.

– At $0.2 < x < 0.89$ samples $La_{0.99-x}Tb_xEu_{0.01}BO_3$ are two-phase, they contain phases of aragonite and vaterite. In the luminescence spectra of ions Eu^{3+} and IR spectra of these samples, bands characteristic of the structures of aragonite $La_{0.99}Eu_{0.01}BO_3$ and vaterite $Tb_{0.99}Eu_{0.01}BO_3$ are observed.

– At $0.89 \le x \le 0.99$ orthoborates have a vaterite structure (SG $P6_3/m$). The luminescence spectra of ions Eu^{3+} contain bands 588–596, 608–613 and 624–632 nm, typical for compounds $Tb_{0.99}Eu_{0.01}BO_3$. In the LES of ions Eu^{3+}, along with the bands characteristic of the vaterite modification of $ReBO_3(Eu)$, where Re = Lu, Y, bands corresponding to the excitation of the luminescence of ions Tb^{3+} are observed. Absorption bands are observed in the IR spectrum of the vaterite phase 565, 695, 868, 921, 999, 1014 and 1049 cm^{-1}.

It was found that with an increase in the concentration of ions Tb^{3+}, the formation of the vaterite phase in samples $La_{0.99-x}Tb_xEu_{0.01}BO_3$, initially having the structure of aragonite, occurs, unlike compounds $LaReBO_3(Eu)$, where $Re = Lu$, Y, simultaneously in the entire volume of microcrystals.

It is shown that the luminescence spectrum of the compound $La_{0.91}Tb_{0.09}BO_3$, having the structure of aragonite, in the wavelength range 535−560 nm contains bands whose maxima are at $\lambda_{max} \sim 540.1$; 541.7; 543.3; 545.1; 546.7; 549.1; 551.3 and 554.7 nm ($^5D_4 \rightarrow {}^7F_5$).

In orthoborates $La_{0.99-x}Tb_xEu_{0.01}BO_3$, as in $La_{0.99-x}Y_xEu_{0.01}BO_3$, band with $\lambda_{ex} = 369$ nm ($^7F_0 \rightarrow {}^5D_2$) in the luminescence excitation spectra (LES) and the band in the wavelength range 577−582 nm ($^5D_0 \rightarrow {}^7F_0$) in the luminescence spectra (LS) of these compounds can serve as indicators of the structural state of the sample. The LES of the samples having the vaterite phase contain the band with $\lambda_{ex} = 369$ nm, while this band is not present in the samples having the aragonite structure. If in the LS the maximum of the band, which corresponds to the $^5D_0 \rightarrow {}^7F_0$ transition, is located at wavelengths shorter than 580 nm, the sample has the aragonite structure, if at λ longer than 580 nm, the sample has the vaterite structure. Two bands with $\lambda_{max} = 578.6$ nm and 580.3 nm corresponding to the transition $^5D_0 \rightarrow {}^7F_0$ were observed for the first time in LS samples containing both aragonite and vaterite phases.

It is shown that when the samples $La_{0.99-x}Tb_xEu_{0.01}BO_3$ are excited in the resonance absorption band of Tb^{3+} ions ($\lambda_{ex} = 378.5$ nm) luminescence of both Tb^{3+} and Eu^{3+} ions is observed simultaneously. With an increase in the concentration of Tb^{3+}, the luminescence intensity of Tb^{3+} initially increases, reaches its maximum at 9 at.%, and then, due to the concentration quenching of the luminescence, at $0.89 \leq x \leq 0.99$, decreases almost to 0. At the same time, the luminescence intensity of ions Eu^{3+} at $\lambda_{ex} = 378.5$ nm continuously increases up to $x = 0.99$. It is established that the maximum luminescence intensity of compounds $Tb_{1-x}Eu_xBO_3$ is observed at a concentration of $Eu^{3+} = 2$ at.%.

It is established that the luminescence of ions Eu^{3+} in orthoborates $La_{0.99-x}Tb_xEu_{0.01}BO_3$ is observed when the sample is excited by light in the absorption bands of ions Tb^{3+}, which indicates the transfer of electron excitation energy from ions Tb^{3+} to ions Eu^{3+}. The efficiency of this process in samples of $La_{0.86}Tb_{0.09}Eu_{0.05}BO_3$ having the structure of aragonite is 86%.

Orthoborates $La_{0.99-x}Tb_xEu_{0.01}BO_3$ have high luminescence intensity, radiation and chemical stability and can be used as effective red phosphors for LED light sources.

Acknowledgments

The authors thank the Research Facility Center of ISSP RAS for the morphology study of the samples and their characterization by IR spectroscopy and X-ray diffraction analysis methods.

Funding

The work has been performed under the state assignment of ISSP of RAS.

Conflict of interest

The authors declare that they have no conflict of interest.

References

[1] M. Balcerzyk, Z. Gontarz, M. Moszynski, M. Kapusta. J. Lumin. **87-89**, 963 (2000).
[2] V.V. Mikhailin, D.A. Spassky, V.N. Kolobanov, A.A. Meotishvili, D.G. Permenov, B.I. Zadneprovski. Rad. Meas. **45**, 307 (2010).
[3] G. Blasse, B.C. Grabmaier. Luminescent Materials. Berlin–Heiderberg, Springer–Verlag (1994). 233 p.
[4] C. Mansuy, J.M. Nedelec, C. Dujardin, R. Mahiou. Opt. Mater. **29**, *6*, 697 (2007).
[5] Jun Yang, Chunxia Li, Xiaoming Zhang, Zewei Quan, Cuimiao Zhang, Huaiyong Li, Jun Lin. Chem. Eur. J. **14**, *14*, 4336 (2008).
[6] S.Z. Shmurak, V.V. Kedrov, A.P. Kiselev, T.N. Fursova, I.I. Zver'kova. FTT **62**, *12*, 2110 (2020). (in Russian).
[7] S.Z. Shmurak, V.V. Kedrov, A.P. Kiselev, T.N. Fursova, I.I. Zver'kova, E.Yu. Postnova. FTT **63**, *10*, 1617 (2021). (in Russian).
[8] J. Yang, G. Zhang, L. Wang, Z. You, S. Huang, H. Lian, J. Lin. J. Solid State Chem. **181**, *12*, 2672 (2008).
[9] S.Z. Shmurak, V.V. Kedrov, A.P. Kiselev, T.N. Fursova, I.M. Shmyt'ko. FTT **57**, *8*, 1558 (2015). (in Russian).
[10] S.Z. Shmurak, V.V. Kedrov, A.P. Kiselev, T.N. Fursova, I.I. Zver'kova. FTT **64**, *1*, 105 (2022). (in Russian).
[11] E. Nakazawa, S. Shianoya. J. Chem. Phys. **47**, 3211 (1967).
[12] B. Di Bartolo, G. Armagan, M. Buoncristiani. Opt. Mater. **4**, *1*, 11 (1994).
[13] M. Inokuti, F. Yirayama. J. Chem. Phys. **43**, *6*, 1978 (1965).
[14] V.M. Agranovich, M.D. Galanin. Perenos energii elektronnogo vozbuzhdeniya v kondensirovannykh sredakh. Nauka, M. (1978). 383 p. (in Russian).
[15] I.A. Bondar, A.I. Burstein, A.V. Krutikov, L.M. Mezentseva, V.V. Osiko, V.P. Sakun, V.A. Smirnov, I.A. Shcherbakov. ZhETF **81**, 96 (1981). (in Russian).
[16] S.K. Sekatskiy, V.S. Letokhov. Pis'ma v ZhETF **63**, *5*, 311 (1996). (in Russian).
[17] S.Z. Shmurak, V.V. Kedrov, A.P. Kiselev, T.N. Fursova, I.M. Shmyt'ko. FTT **58**, *3*, 564 (2016). (in Russian).
[18] S.Z. Shmurak, V.V. Kedrov, A.P. Kiselev, T.N. Fursova, O.G. Rybchenko. FTT **59**, *6*, 1150 (2017). (in Russian).
[19] S.Z. Shmurak, V.V. Kedrov, A.P. Kiselev, T.N. Fursova, O.G. Rybchenko. FTT **61**, *1*, 123 (2019). (in Russian).
[20] S.Z. Shmurak, V.V. Kedrov, A.P. Kiselev, T.N. Fursova, I.I. Zver'kova, S.S. Khasanov. FTT **62**, *11*, 1888 (2020). (in Russian).
[21] Y. Jin, Y. Hu, L. Chen, X. Wang, Z. Mu, G. Ju, Z. Yang. Physica B **436**, 105 (2014).

[22] Z.J. Hang, H.H. Chen, X.X. Yang, J.T. Zhao. Mater. Sci. Eng. B **145**, *1–3*, 34 (2007).
[23] W.W. Holloway, M. Kestigian, R. Newman. Phys. Rev. Lett. **11**, *10*, 458 (1963).
[24] J. Yang, G. Li, C. Peng, C. Li, C. Zhang, Y. Fan, Z. Xu, Z. Cheng, J. Lin. J. Solid State Chem. **183**, *2*, 451 (2010).
[25] G. Garsia-Rosales, F. Mersier-Bion, R. Drot, G. Lagarde, J. Rogues, E. Simoni. J. Lumin. **132**, *5*, 1299 (2012).
[26] X. Zhang, Z. Zhao, X. Zhang, A. Marathe, D.B. Cordes, B. Weeks, J. Chaudhuri. J. Mater. Chem. C, **1**, *43*, 7202 (2013).
[27] J. Thakur, D.P. Dutta, H. Bagla, A.K. Tyagi. J. Am. Ceram. Soc. **95**, *2*, 696 (2012).
[28] Heng-Wei Wei, Li-Ming Shao, Huan Jiao, Xi-Ping Jing. Opt. Mater. **75**, 442 (2018)
[29] J. Hölsä. Inorg. Chim. Acta **139**, *1–2*, 257 (1987).
[30] G. Chadeyron, M. El-Ghozzi, R. Mahiou, A. Arbus, C. Cousseins. J. Solid State Chem. **128**, 261 (1997).
[31] R.S. Roth, J.L. Waring, E.M. Levin. Proc. 3rd. Conf. Rare Earth Res. Clearwater, Fla. (1964). P. 153.
[32] E.M. Levin, R.S. Roth, J.B. Martin. Am. Miner. **46**, *9–10*, 1030 (1961).
[33] C. Badan, O. Esenturk, A. Yelmaz. Solid State Sci. **14**, *11–12*, 1710 (2012).
[34] I.M. Shmyt'ko, I.N. Kiryakin, G.K. Strukova. FTT **55**, *7*, 1369 (2013). (in Russian).
[35] N.I. Steblevskaya, M.I. Belobeletskaya, M.A. Medkov. Zhurn. neorgan. khimii **66**, *4*, 440 (2021). (in Russian).
[36] Ling Li, Shihong Zhou, Siyuan Zhang. Solid State Sci. **10**, 1173 (2008).
[37] A. Szczeszak, T. Grzyb, St. Lis, R.J. Wiglusz. Dalton Transactions **41**, 5824 (2012).
[38] S.Z. Shmurak, V.V. Kedrov, A.P. Kiselev, T.N. Fursova, I.I. Zver'kova, S.S. Khasanov. FTT **63**, *12*, 2142 (2021). (in Russian).
[39] S.Z. Shmurak, V.V. Kedrov, A.P. Kiselev, T.N. Fursova, I.I. Zver'kova. FTT **64**, *4*, 474 (2022). (in Russian).
[40] A. Haberer, R. Kaindl, H. Huppertz. Z. Naturforsch. B **65**, 1206 (2010).
[41] R. Velchuri, B.V. Kumar, V.R. Devi, G. Prasad, D.J. Prakash, M. Vital. Mater. Res. Bull. **46**, *8*, 1219 (2011).
[42] Jin Teng-Teng, Zhang Zhi-Jun, Zhang Hui, Zhao Jing-Tai. J. Inorganic Mater. **28**, *10*, 1153 (2013).
[43] S.Z. Shmurak, V.V. Kedrov, A.P. Kiselev, T.N. Fursova, I.I. Zver'kova. FTT **64**, *8*, 955 (2022). (in Russian).
[44] A.G. Ryabukhin. Izv. Chelyabinskogo nauch. tsentra **4**, 33 (2000). (in Russian).
[45] C.E. Weir, E.R. Lippincott. J. Res. Natl. Bur. Std. A **65A**, *3*, 173 (1961).
[46] W.C. Steele, J.C. Decius. J. Chem. Phys. **25**, *6*, 1184 (1956).
[47] J.P. Laperches, P. Tarte. Spectrochim. Acta **22**, 1201 (1966).
[48] J.H. Denning,S.D. Ross. Spectrochim. Acta **28A**, 1775 (1972).
[49] Guang Jia, Cuimiao Zhang, Chunzheng Wang, Lei Liu, Cuimiao Huang, Shiwen Ding. Cryst. Eng. Commun. **14**, 579 (2012).
[50] Guang Jia, Jing-Yi Liu, Dong-Bing Dong, Cui-Miao Zhang. Adv. Mater. Res. **1052**, 193 (2014).